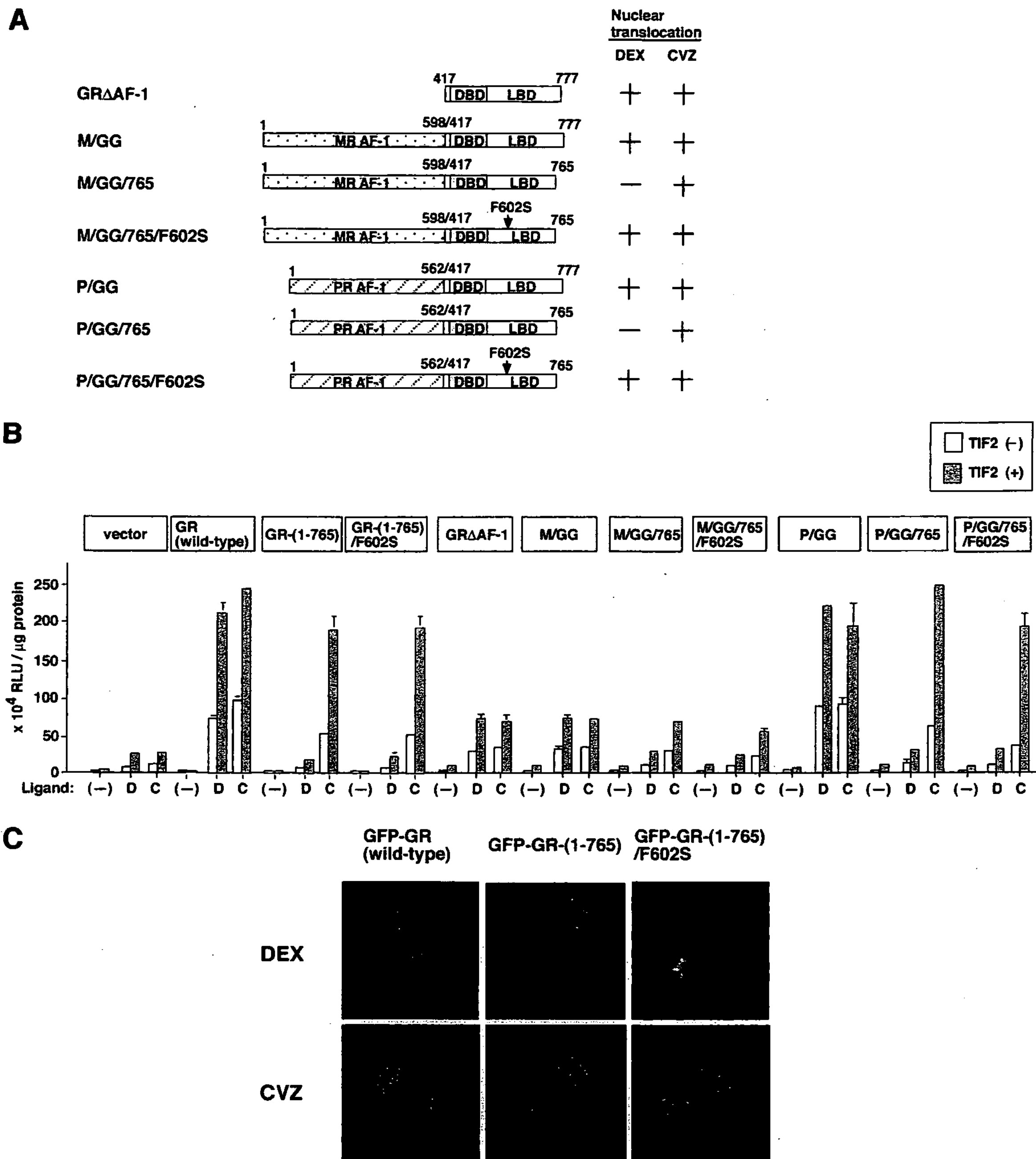

Fig. 5. Role of Ligands and AF-1 in Functional Interaction between the LBD of C-Terminally Truncated GR and TIF2

A, Schematic illustration of AF-1 deleted GR and AF-1-chimeric receptors. GRΔAF-1 lacks N-terminal domain containing AF-1 of the GR. MR AF-1 and PR AF-1, the N-terminal domain containing AF-1 of the human MR and PR B form, were fused to GRΔAF-1, and resultant chimeric receptors are designated as M/GG and P/GG, respectively. M/GG/765 and P/GG/765 are C-terminally 12 amino acid-truncated form of the M/GG and P/GG, respectively. M/GG/765/F602S and P/GG/765/F602S contain additional F602S amino acid substitution (*arrowheads*) in M/GG/765 and P/GG/765, respectively. Ligand-dependent nuclear translocation of these chimeric proteins was examined with indirect immunofluorescence assay as described in *Materials and Methods*. B, Effects of exogenous expression of TIF2 on DEX- and CVZ-dependent GRE-driven reporter gene expression by C-terminally truncated, AF-1 truncated, or AF-1-chimeric GR. COS7 cells were cotransfected with 2 μg of pGRE-LUC and 100 ng of either empty vector pCMX or expression plasmids for wild-type GR, GR-(1–765), GR-(1–765)/F602S, GRΔAF-1, or their AF-1-chimeric receptors with or without 600 ng of expression plasmid for TIF2 as indicated, and cultured in the presence or absence of 1 μM of DEX (D) or CVZ (C) for 24 h. Experiments were performed in triplicate and results are expressed as relative light units (RLU) per microgram of protein in the extract, and the means ± SD are shown. C, Effects of DEX and CVZ on the subnuclear colocalization of the C-terminal truncated GR with TIF2. GFP-tagged wild-type GR, GR-(1–765), or GR-(1–765)/F602S was transiently expressed with TIF2 in COS7 cells and the cells were cultured in the presence or absence of 1 μM of DEX or CVZ for 2 h. Then digital images were taken as described in *Materials and Methods* and representative results are shown.

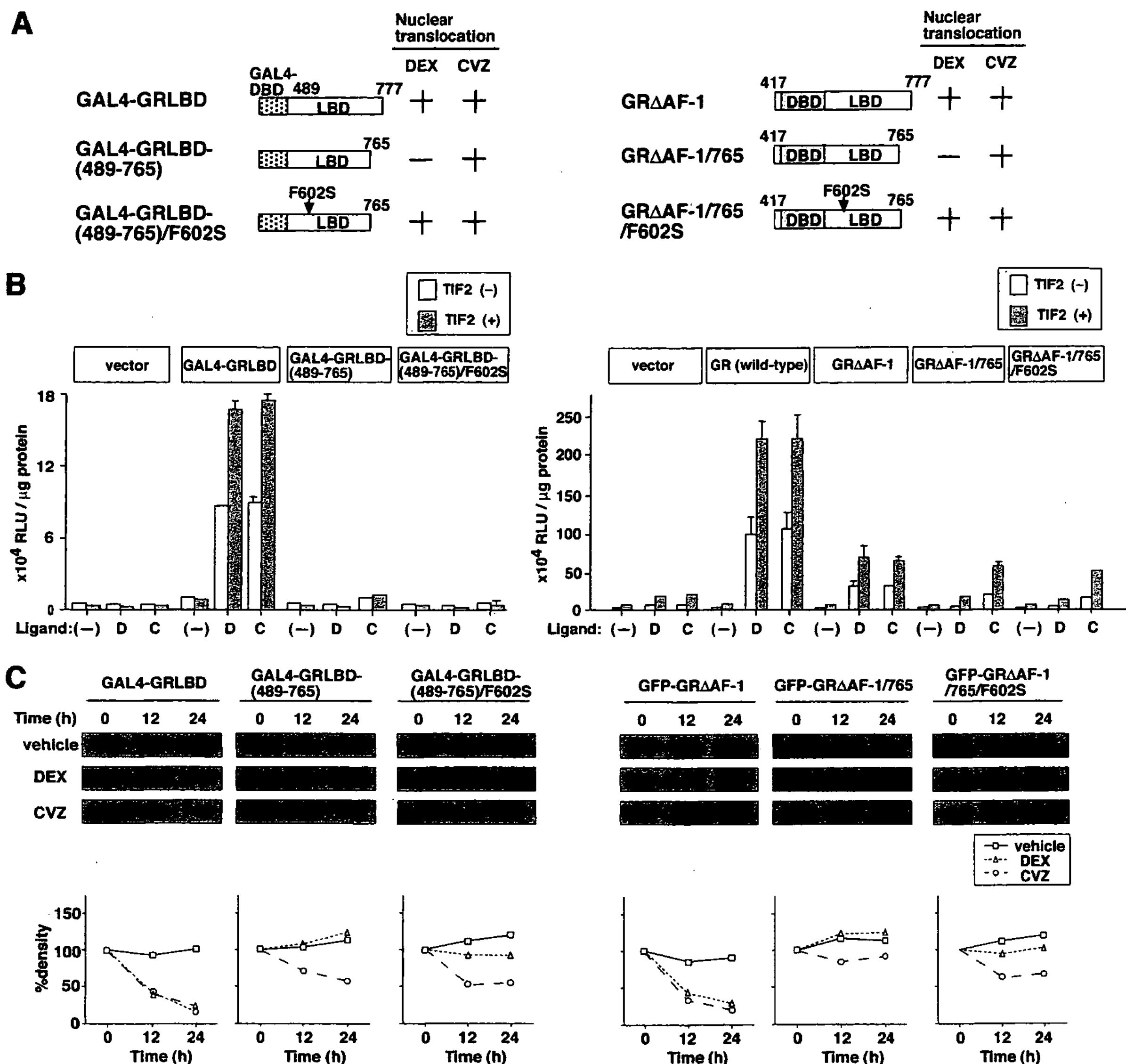

Fig. 6. Cooperation of the DBD in Ligand-Dependent Coactivator Recruitment of the LBD

A, Schematic illustration and subcellular localization of the GR LBD fused to the DBD of the GAL4 or GR and their C-terminally truncated mutants. GAL4-GRLBD (*left*), GRΔAF-1 (*right*), and their C-terminally truncated mutants are schematically illustrated. Ligand-dependent nuclear translocation of these chimeric proteins was examined with indirect immunofluorescence assay as described in *Materials and Methods*. B, Role of the DBD on the ligand-dependent interaction between the LBD and TIF2 in the GR. For modified one-hybrid assay, COS7 cells were cotransfected with 2 μg of the GAL4-driven reporter plasmid tk-GALpx3-LUC (*left*) or GRE-driven reporter plasmid pGRE-LUC (*right*) and 100 ng of either empty vector pCMX or expression plasmids for GAL4-GRLBD (*left*), GRΔAF-1 (*right*), or their mutants with or without 600 ng of expression plasmid for TIF2 as indicated. After further 24 h of culture in the presence or absence of 1 μM of DEX (D) or CVZ (C), the cells were harvested and luciferase activities were measured as described in *Materials and Methods*. Experiments were performed in triplicate and results are expressed as relative light units (RLU) per microgram of protein in the extract and the means ± SD are shown. C, Expression levels of GAL4-GRLBD, GRΔAF-1 and their C-terminally truncated mutants. COS7 cells were transiently transfected with expression plasmid for GAL4-GRLBD (*left*), GRΔAF-1 (*right*), or their C-terminally truncated mutants as indicated. The cells were further cultured and treated with vehicle or 1 μM of DEX or CVZ for 0, 12, or 24 h. Whole cell extracts were prepared and 10 μg of protein was separated by SDS-PAGE. Expression levels of each protein were analyzed by Western immunoblotting using anti-GAL4 (DBD) or anti-GFP antibodies as described in *Materials and Methods*. Data were quantitated as described in *Materials and Methods* and expressed as percentage of density, which is given relative to the density obtained from the cells before addition of ligands (0 h). Experiments were repeated three times with almost identical results, and representative results are shown.

flexible and can adapt to different sized ligands. When compared with the small agonist T0901317, the larger agonist GW3965 shifts many side-chains and enlarges the volume of the ligand binding pocket. This results in a different local conformation in a sector of the LBD while preserving the interaction between the ligand

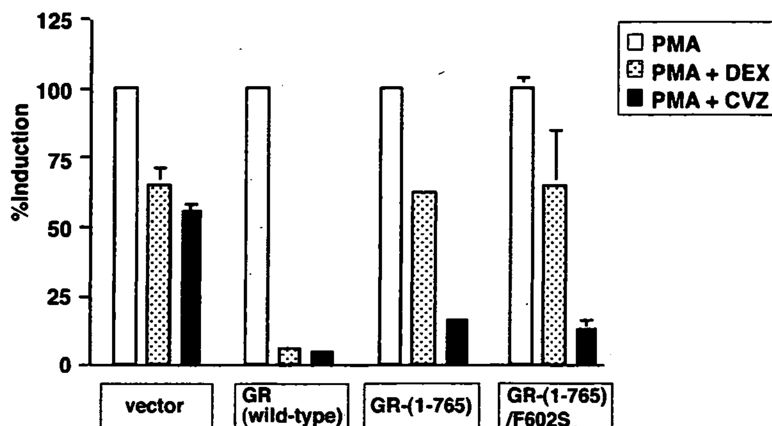

Fig. 7. CVZ Elicits Transrepression Function of the GR Despite the Lack of the C-Terminal End

HeLa cells were cotransfected with 2 μg of pNFκBHL reporter plasmid and 1 μg of either empty vector pCMX or expression plasmids for the wild-type GR, GR-(1–765), or GR-(1–765)/F602S. The cells were cultured and treated with or without 10 nM phorbol 12-myristate acetate (PMA) in the presence or absence of 1 μM of DEX or CVZ for 24 h. Assays were performed in triplicate and results are expressed as percentage of induction, which is given relative to the luciferase activity obtained from the cells treated with PMA alone, and the means ± SD are shown.

and helix 12 intact (40). In our model, the bulky A-ring of CVZ intimately contacts with and modulates the conformation of helices 3 and 5 (Fig. 1). Along this line, Ali *et al.* (41) have reported on compounds that have a phenylpyrazole group at the A-ring. Replacement of the C- and D-ring of the steroid backbone by alkyl, alkenyl, or benzyl groups yields compounds that selectively bind to the GR and induce transactivation (41). As in the case of CVZ and DEX, when the phenylpyrazole group in such compounds is replaced by a C3-ketone, their GR binding ability is completely abolished (41). This suggests that the mode of binding between these compounds is similar and is consistent with the idea that contacts between the phenylpyrazole A-ring and helices 3 and 5 are compatible with a stable active conformation. Interestingly, a similar modeling and functional approach in the MR argues that the Ser-810 to Leu substitution in helix 5 of the MR, which renders progesterone and the antagonist spironolactone into an agonist, is due to the creation of new interactions between these ligands and helices 3 and 5 (42). Concerning the GR, the conformation of helix 3 is likely to be important for agonism because Lys-579 within this helix is involved in clamping the C-terminal end of the coactivator helix and mutation of this residue reduces GR transactivation without affecting ligand binding (15, 31).

The C-terminal end of the GR LBD forms an extended β-sheet that is important for binding of certain agonists and stable interaction with coactivators (15, 16, 38, 43). Deletion of the C-terminal 12 amino acids from GR severely compromises the ability of DEX to bind, to induce a trypsin-resistant conformation of the LBD, and to support transactivation. Because this deletion does not extend into the AF-2 helix and preserves the essential constituents of the AF-2 pocket, the observations suggest that the role of these residues is to stabilize an active conformation of the receptor. Our current results indicate that the deleterious effects of this deletion can be surmounted when CVZ occupies the binding pocket. This indicates that the deleted receptor possesses all the necessary features for an active conformation as long as an appropriate ligand is bound. In this view, it is likely that the additional contacts provided by the bulky phenylpyrazole substituent yield a stable active conformation without the contributions provided by the C-terminal residues. The fact that the stabilizing F602S substitution can restore the ability of DEX to bind and induce the nuclear translocation of the C-terminally deleted GR is also consistent with CVZ stabilizing an active conformation. The fact that DEX-dependent transcriptional activity of the deletion mutants is not restored by the F602S mutation suggests that, in this context, the stabilizing influence of the F602S is not sufficient and that conformations other than an active one are favored. A similar behavior is also observed in the case of the antagonist RU486 because it is capable of binding and inducing the nuclear translocation of GR even after deletion of the last 28 C-terminal amino acids (44, 45). Our results, thus, clearly show that the C-terminal 12 amino acids are not absolutely essential for agonistic activity and highlight the critical role played by the ligand in sculpting the functional surfaces of the receptor.

The unique ability of CVZ to support transactivation by the C-terminally deleted receptor allowed us to examine the role played by domains other than the LBD. Our results indicate that, at least in terms of ligand-dependent transactivation, the N-terminal region of the receptor is not essential but contributes to overall activity, most likely through cooperation between AF-1 and AF-2 (46). More importantly, direct targeting of the C-terminally deleted LBD to the DNA via the GAL4 DBD does not support CVZ-driven activity and TIF-2 recruitment. In contrast, when the de-

leted LBD is brought to the promoter by the GR's own DBD, CVZ is able to support transactivation and TIF-2 recruitment. Together with the protease digestion studies, these results indicate that, although CVZ can promote a trypsin-resistant conformation of the C-terminally deleted LBD alone, the transcriptional effects of CVZ require the DBD of GR. The unique role of the GR DBD might involve an appropriate orientation of the two LBDs upon DNA binding-induced dimerization or more likely, reflects a direct contribution of the DBD to the active conformation of the CVZ-bound LBD. Several laboratories have shown that the DBD stabilizes the LBD and enhances ligand-dependent nuclear translocation (47–50). Moreover, ligand-driven conformations of the LBD can influence both DNA binding (51) and anti-NF-κB activities (52). Kumar *et al.* (53) have suggested that the DBD plays an important role in the structural stabilization of the GR. Importantly, interdomain communication is not exclusive to GR and has been observed in other receptors as well, especially in AR (54). Steroid pharmacology is increasingly focused in the development of ligands with selective modulatory activities. Because the mode of interdomain communication may be distinct for each receptor and may be modulated in a ligand-, tissue-, and promoter-context-dependent manner, ligands such as CVZ and other phenylpyrazole analogs that manipulate this regulatory avenue will not only provide a better understanding of the mechanisms of interdomain communication but also provide novel leads in the development of selective GR modulators.

MATERIALS AND METHODS

Reagents and Antibodies

DEX was purchased from Sigma (St. Louis, MO). CVZ was a kind gift from Aventis Pharma (Strasbourg, France). Other chemicals were obtained from Wako Pure Chemical (Osaka, Japan) unless otherwise specified. Monoclonal anti-hsp90 antibodies were obtained from Affinity Bioreagents, Inc. (Golden, CO). Goat antimouse IgM and control mouse IgM TEPC183 were obtained from Sigma. Monoclonal anti-GFP antibodies were obtained from CLONTECH (Palo Alto, CA). Polyclonal anti-GAL4 (DBD) and antipolyhistidine antibodies were obtained from Santa Cruz Biotechnologies (Santa Cruz, CA).

Plasmids

The expression plasmids for the wild-type and C-terminal 12 amino acid-truncated human GR, pCMX-GR, and pCMX-GR-(1–765) have been previously described (26). Construction of pCMX-GR-(1–765)/F602S was carried out using the QuikChange site-directed mutagenesis kit (Stratagene, La Jolla, CA) using pCMX-GR-(1–765) as a template. The expression plasmids for the fusion between the simian virus 40 NLS and the human GR LBD (amino acids 499–777) and for the fusion of GFP and wild-type human GR, pCMX-NLS-GRLBD and pCMX-GFP-GR have been previously described (55, 56). The expression plasmid for the chimera between the GAL4 DBD and the human GR LBD (amino acids 489–777), pCMX-GAL4-GRLBD, was a kind gift of Dr. K. Umesono (Kyoto University, Kyoto, Japan). To construct the expression plasmid for GFP- or polyhistidine-tagged AF-1-deleted human GR (amino acids 417–777), pCMX-GFP-GRΔAF-1 or pCMX-GRΔAF-1, the DNA fragments encoding human GR DBD and LBD were inserted into the parent pCMX-GFP or pCMX-6xHis vectors, respectively. To construct the expression plasmids for chimeric proteins of the AF-1 of either the human MR (amino acids 1–598) or PR B form (amino acids 1–562) and GRΔAF-1 (resultant plasmids are pCMX-MRAF-1/GRΔAF-1 and pCMX-PRBAF-1/GRΔAF-1, respectively), the N-terminal domain of each receptor was amplified by PCR using pRShMR or pEGFP-PRB as templates with appropriate flanking sequences [these template plasmids were a kind gift of Dr. R. M. Evans (Salk Institute, La Jolla, CA) and Dr. G. L. Hager (National Cancer Institute, Bethesda, MD), respectively], and inserted into the parent pCMX-GRΔAF-1. To exchange the mutations within the LBD, *PstI-BamHI* fragments encoding a part of the human GR LBD (amino acids 596–765) from pCMX-GR-(1–765) or pCMX-GR-(1–765)/F602S were inserted into the same sites of the recipient expression plasmids. The expression plasmid for TIF2 pSG5-TIF2 was kindly provided by Dr. P. Chambon (Institut de Genetique et de Biologie Moleculaire et Cellulaire, Strasbourg, France). The GRE-driven reporter plasmid pGRE-LUC, GAL4-responsive reporter plasmid tk-GALpx3-LUC, and NF-κB-responsive reporter plasmid pNFκBHL have been described previously (57).

Cell Culture and Heat Shock Treatment

COS7 and HeLa cells were obtained from the RIKEN Cell Bank (Tsukuba, Japan) and maintained in DMEM (Sigma) supplemented with 10% fetal calf serum and antibiotics. In all experiments, serum steroids were stripped with dextran-coated charcoal, and cells were cultured in a humidified atmosphere at 37 C with 5% CO_2. Heat shock treatment for COS7 cells was achieved by shifting flasks to another 5% CO_2 incubator set at 43 C.

Graphical Manipulations and Ligand Docking

Graphical manipulations were performed using SYBYL 6.9 (Tripos, St. Louis, MO). The atomic coordinates of the crystal structure of human GR LBD (amino acids 523–777) were retrieved from Protein Data Bank (entry 1M2Z) (15). We docked CVZ into the ligand binding pocket manually by superimposing its steroid backbone with that of DEX (58–60). Energy minimization of CVZ/GR-LBD complex was performed until the energy gradient was lower than 0.1 kcal/(mol)(Å) on Tripos force field by using subset minimization command.

Immunoprecipitation and Western Immunoblot Assay

For analysis of the interaction between the GR and hsp90, we transiently transfected expression plasmids for wild-type GR or its mutants in COS7 cells and the assays were performed as described previously (56). In brief, whole cell extracts were prepared by lysing cells and immunoprecipitating with either the anti-hsp90 IgM antibody 3G3 or control mouse IgM antibody TEPC 183 as follows. We first prepared goat antimouse IgM coupled to CNBr-activated Sepharose 4B (Amersham Biosciences, Piscataway, NJ) as described previously (56). Seventy micrograms of cellular protein was added to the goat antimouse IgM-coupled Sepharose. The reaction mixtures were incubated on ice for 90 min, after which Sepharose beads were pelleted by centrifugation and washed three times with MENG buffer [25 mM Mops (pH 7.5), 1 mM EDTA, 0.02% NaN_3, 10% glycerol] containing 20 mM sodium molybdate and 2 mM dithiothreitol. Immunoprecipitated proteins were eluted by boiling in sample buffer and

analyzed by SDS-PAGE and electrophoretically transferred to an Immobilon-NC Pure nitrocellulose membrane (Millipore, Bedford, MA). Subsequently, Western immunoblot analysis was performed with polyclonal anti-GR antibodies diluted at 1:1000, followed by horseradish peroxidase-conjugated antirabbit Ig (Amersham Biosciences) diluted at 1:2000. After stripping off the immune complexes, the same membrane was probed for detection of hsp90, using monoclonal mouse anti-hsp90 IgG antibodies 3B6 (1:500), followed by horseradish peroxidase-conjugated antimouse Ig diluted at 1:1000. In parallel, 20 μg of whole cell extracts were independently used for immunodetection of wild-type and mutant GR or hsp90. Antibody-protein complexes were visualized using the enhanced chemiluminescence method according to the manufacturer's protocol (Amersham Biosciences).

Visualization of GFP Fusion Proteins

For analysis of subcellular localization of the human GR and its mutants, we transiently expressed GFP-tagged receptors in COS7 cells and assays were performed as described previously (26). Briefly, after 6 h of transient transfection of the expression plasmids for GFP-fusion proteins, the medium was replaced with phenol red-free DMEM supplemented with 2% dextran-coated charcoal-treated fetal calf serum, and the cells were cultured at 37 C for at least 24 h. After various treatments, cells were examined using an IX70 microscope (Olympus, Tokyo, Japan) enclosed by an incubator and equipped with a heating-stage and a fluorescein isothiocyanate filter set. Digital images were randomly taken in eight views and analyzed on FLUOVIEW FV 500 systems (Olympus).

Limited Proteolysis Assay

The expression plasmids for the GR and its mutants, which contain the coding sequences under control of the T7 promoter, were transcribed and translated with the TNT^{T7}-coupled reticulocyte lysate system (Promega Corp., Madison, WI) in the presence of [^{35}S]Met (1000 Ci/mmol, Amersham Biosciences) according to the manufacturer's instruction. Three microliters of [^{35}S]Met-labeled translation mixtures including *in vitro*-translated GR were incubated for 30 min at 20 C with 1 μl of vehicle (0.4% ethanol) or 10 μM of DEX or CVZ. Limited proteolysis was performed by the addition of 1 μl of trypsin solution to the translation mixtures (final trypsin concentrations were 5–100 μg/ml). Digestion was conducted for 10 min at 20 C and stopped by cooling in ice, followed by the addition of 5 μl of sodium dodecyl sulfate (SDS) sample buffer and boiling for 5 min. The proteolysis products were separated on a 1.5-mm thick 12% SDS-polyacrylamide gels. After electrophoresis, the gels were vacuum-dried for 60 min at 80 C and autoradiographed.

Transfection and Reporter Gene Assay

Cells were plated on 6-cm diameter culture dishes (Iwaki Glass, Chiba, Japan) to 30–50% confluence and cell culture medium was replaced with Opti-MEM lacking phenol red (Invitrogen, Carlsbad, CA) before transfection. Plasmid cocktail was mixed with TransIT-LT1 transfection reagent (Panvera Corp., Madison, WI) and added to the culture. Total amount of the plasmids was kept constant by adding an irrelevant plasmid (pGEM3Z was used unless otherwise specified). After 6 h of incubation, the medium was replaced with fresh DMEM supplemented with 2% dextran-coated charcoal-treated fetal calf serum, and the cells were cultured in the presence or absence of various ligands for 24 h at 37 C. Luciferase enzyme activity was determined using a luminometer (Promega) essentially as described (26).

Indirect Immunofluorescence Assay

For assessment of subcellular localization of chimeric GR proteins, indirect immunofluorescence assay was performed as described previously (26). After transfection of expression plasmids for various GR mutants into COS7 cells, the cells were grown on eight-chambered sterile glass slides (Nippon Becton Dickinson, Tokyo, Japan) for 24 h and were treated without or with I μM of DEX or CVZ for 2 h. The cells were fixed in ice-cold acetone for 2 min and air-dried. After fixation, the cells were washed with PBS and incubated with anti-GR polyclonal rabbit antibody at a dilution of 1:100 in PBS containing 0.1% Triton X-100 for 1 h at 37 C. Then, the cells were washed three times with PBS and incubated with fluorescein isothiocyanate-conjugated antirabbit IgG (Santa Cruz Biotechnology) at a dilution of 1:200 in PBS containing 0.1% Triton X-100 for 1 h at 37 C. The cells were finally washed three times with PBS and mounted with GEL/MOUNT (Biomeda Corp., Foster City, CA) for examination on a confocal laser-scanning microscope IX70. Digital images were randomly taken in eight views and analyzed on FLUOVIEW FV 500 systems.

Quantitative Analysis of Chimeric Proteins

For determination of expression levels of GFP-, GAL4-, and polyhistidine-tagged proteins, we transiently expressed each chimeric protein in COS7 cells and the cells were cultured in the presence or absence of ligands for 0, 12, or 24 h. After various treatments, whole cell extracts were prepared and 10 μg of proteins ware separated by SDS-PAGE and transferred to nitrocellulose membranes. Subsequently, Western immunoblot analysis was performed with anti-GFP, -GAL4 (DBD), and -polyhistidine antibodies followed by appropriate secondary horseradish peroxidase-conjugated antibodies. Antibody-protein complexes were visualized using the enhanced chemiluminescence method. Expression levels of each chimeric protein were quantified by scanning the blot and using image analysis software from the National Institutes of Health (NIH Image 1.62).

Acknowledgments

We thank Drs. H. Ogawa, P. Chambon, R. M. Evans, G. L. Hager, and K. Umesono for plasmids and the members of Morimoto laboratory for fruitful discussions and help.

Received June 30, 2004. Accepted January 20, 2005.

Address all correspondence and requests for reprints to: Hirotoshi Tanaka, M.D., Ph.D., the Division of the Clinical Immunology, the Advanced Clinical Research Center, the Institute of Medical Science, the University of Tokyo, 4-6-1, Shirokanedai, Minato-ku, Tokyo 108-8639, Japan. E-mail: hirotnk@ims.u-tokyo.ac.jp.

This work was supported in part by the grants from the Ministry of Education, Science, Technology, Sports, and Culture, the Ministry of Health, Labour, and Welfare, the Takeda Science Foundation, the Uehara Memorial Foundation, the Vehicle Racing Commemorative Foundation, and Japan Society for the Promotion of Science.

REFERENCES

1. Sapolsky RM, Romero LM, Munck AU 2000 How do glucocorticoids influence stress responses? Integrating permissive, suppressive, stimulatory, and preparative actions. Endocr Rev 21:55–89

2. Reichardt HM, Tronche F, Berger S, Kellendonk C, Schutz G 2000 New insights into glucocorticoid and mineralocorticoid signaling: lessons from gene targeting. Adv Pharmacol 47:1–21
3. Adcock IM 2003 Glucocorticoids: new mechanisms and future agents. Curr Allergy Asthma Rep 3:249–257
4. Resche-Rigon M, Gronemeyer H 1998 Therapeutic potential of selective modulators of nuclear receptor action. Curr Opin Chem Biol 2:501–507
5. Miner JN 2002 Designer glucocorticoids. Biochem Pharmacol 64:355–361
6. Mangelsdorf DJ, Thummel C, Beato M, Herrlich P, Schutz G, Umesono K, Blumberg B, Kastner P, Mark M, Chambon P, Evans RM 1995 The nuclear receptor superfamily: the second decade. Cell 83:835–839
7. Nuclear Receptors Nomenclature Committee 1999 A unified nomenclature system for the nuclear receptor superfamily. Cell 97:161–163
8. Beato M, Herrlich P, Schutz G 1995 Steroid hormone receptors: many actors in search of a plot. Cell 83: 851–857
9. Bourguet W, Germain P, Gronemeyer H 2000 Nuclear receptor ligand-binding domains: three-dimensional structures, molecular interactions and pharmacological implications. Trends Pharmacol Sci 21:381–388
10. Rosenfeld MG, Glass CK 2001 Coregulator codes of transcriptional regulation by nuclear receptors. J Biol Chem 276:36865–36868
11. Pratt WB, Toft DO 1997 Steroid receptor interactions with heat shock protein and immunophilin chaperones. Endocr Rev 18:306–360
12. Freeman BC, Yamamoto KR 2001 Continuous recycling: a mechanism for modulatory signal transduction. Trends Biochem Sci 26:285–290
13. McKay LI, Cidlowski JA 1999 Molecular control of immune/inflammatory responses: interactions between nuclear factor-κ B and steroid receptor-signaling pathways. Endocr Rev 20:435–459
14. De Bosscher K, Vanden Berghe W, Haegeman G 2003 The interplay between the glucocorticoid receptor and nuclear factor-κB or activator protein-1: molecular mechanisms for gene repression. Endocr Rev 24: 488–522
15. Bledsoe RK, Montana VG, Stanley TB, Delves CJ, Apolito CJ, McKee DD, Consler TG, Parks DJ, Stewart EL, Willson TM, Lambert MH, Moore JT, Pearce KH, Xu HE 2002 Crystal structure of the glucocorticoid receptor ligand binding domain reveals a novel mode of receptor dimerization and coactivator recognition. Cell 110:93–105
16. Kauppi B, Jakob C, Farnegardh M, Yang J, Ahola H, Alarcon M, Calles K, Engstrom O, Harlan J, Muchmore S, Ramqvist AK, Thorell S, Ohman L, Greer J, Gustafsson JA, Carlstedt-Duke J, Carlquist M 2003 The three-dimensional structures of antagonistic and agonistic forms of the glucocorticoid receptor ligand-binding domain: RU-486 induces a transconformation that leads to active antagonism. J Biol Chem 278:22748–22754
17. Onate SA, Tsai SY, Tsai MJ, O'Malley BW 1995 Sequence and characterization of a coactivator for the steroid hormone receptor superfamily. Science 270: 1354–1357
18. Voegel JJ, Heine MJ, Zechel C, Chambon P, Gronemeyer H 1996 TIF2, a 160 kDa transcriptional mediator for the ligand-dependent activation function AF-2 of nuclear receptors. EMBO J 15:3667–3675
19. Hong H, Kohli K, Trivedi A, Johnson DL, Stallcup MR 1996 GRIP1, a novel mouse protein that serves as a transcriptional coactivator in yeast for the hormone binding domains of steroid receptors. Proc Natl Acad Sci USA 93:4948–4952
20. Arany Z, Sellers WR, Livingston DM, Eckner R 1994 E1A-associated p300 and CREB-associated CBP belong to a conserved family of coactivators. Cell 77:799–800
21. Robyr D, Wolffe AP, Wahli W 2000 Nuclear hormone receptor coregulators in action: diversity for shared tasks. Mol Endocrinol 14:329–347
22. Ford J, McEwan IJ, Wright AP, Gustafsson JA 1997 Involvement of the transcription factor IID protein complex in gene activation by the N-terminal transactivation domain of the glucocorticoid receptor *in vitro*. Mol Endocrinol 11:1467–1475
23. Kumar R, Lee JC, Bolen DW, Thompson EB 2001 The conformation of the glucocorticoid receptor af1/τ1 domain induced by osmolyte binds co-regulatory proteins. J Biol Chem 276:18146–18152
24. Hittelman AB, Burakov D, Iniguez-Lluhi JA, Freedman LP, Garabedian MJ 1999 Differential regulation of glucocorticoid receptor transcriptional activation via AF-1-associated proteins. EMBO J 18:5380–5388
25. Schlechte JA, Simons Jr SS, Lewis DA, Thompson EB 1985 [3H]cortivazol: a unique high affinity ligand for the glucocorticoid receptor. Endocrinology 117:1355–1362
26. Yoshikawa N, Makino Y, Okamoto K, Morimoto C, Makino I, Tanaka H 2002 Distinct interaction of cortivazol with the ligand binding domain confers glucocorticoid receptor specificity: cortivazol is a specific ligand for the glucocorticoid receptor. J Biol Chem 277:5529–5540
27. Garabedian MJ, Yamamoto KR 1992 Genetic dissection of the signaling domain of a mammalian steroid receptor in yeast. Mol Biol Cell 3:1245–1257
28. Allan GF, Leng X, Tsai SY, Weigel NL, Edwards DP, Tsai MJ, O'Malley BW 1992 Hormone and antihormone induce distinct conformational changes which are central to steroid receptor activation. J Biol Chem 267: 19513–19520
29. Benkoussa M, Nomine B, Mouchon A, Lefebvre B, Bernardon JM, Formstecher P, Lefebvre P 1997 Limited proteolysis for assaying ligand binding affinities of nuclear receptors. Recept Signal Transduct 7:257–267
30. Wallace AD, Cidlowski JA 2001 Proteasome-mediated glucocorticoid receptor degradation restricts transcriptional signaling by glucocorticoids. J Biol Chem 276: 42714–42721
31. Keeton EK, Fletcher TM, Baumann CT, Hager GL, Smith CL 2002 Glucocorticoid receptor domain requirements for chromatin remodeling and transcriptional activation of the mouse mammary tumor virus promoter in different nucleoprotein contexts. J Biol Chem 277:28247–28255
32. Rupprecht R, Arriza JL, Spengler D, Reul JM, Evans RM, Holsboer F, Damm K 1993 Transactivation and synergistic properties of the mineralocorticoid receptor: relationship to the glucocorticoid receptor. Mol Endocrinol 7:597–603
33. Caldenhoven E, Liden J, Wissink S, Van de Stolpe A, Raaijmakers J, Koenderman L, Okret S, Gustafsson JA, Van der Saag PT 1995 Negative cross-talk between RelA and the glucocorticoid receptor: a possible mechanism for the antiinflammatory action of glucocorticoids. Mol Endocrinol 9:401–412
34. Ray A, Prefontaine KE 1994 Physical association and functional antagonism between the p65 subunit of transcription factor NF-κ B and the glucocorticoid receptor. Proc Natl Acad Sci USA 91:752–756
35. Scheinman RI, Gualberto A, Jewell CM, Cidlowski JA, Baldwin Jr AS 1995 Characterization of mechanisms involved in transrepression of NF-κ B by activated glucocorticoid receptors. Mol Cell Biol 15:943–953
36. Nissen RM, Yamamoto KR 2000 The glucocorticoid receptor inhibits NFκB by interfering with serine-2 phosphorylation of the RNA polymerase II carboxy-terminal domain. Genes Dev 14:2314–2329
37. McKay LI, Cidlowski JA 1998 Cross-talk between nuclear factor-κ B and the steroid hormone receptors: mechanisms of mutual antagonism. Mol Endocrinol 12:45–56

38. Bledsoe RK, Stewart EL, Pearce KH 2004 Structure and function of the glucocorticoid receptor ligand binding domain. Vitam Horm 68:49–91
39. Li Y, Lambert MH, Xu HE 2003 Activation of nuclear receptors: a perspective from structural genomics. Structure (Camb) 11:741–746
40. Farnegardh M, Bonn T, Sun S, Ljunggren J, Ahola H, Wilhelmsson A, Gustafsson JA, Carlquist M 2003 The three dimensional structure of the liver X receptor β reveals a flexible ligand binding pocket that can accommodate fundamentally different ligands. J Biol Chem 278:38821–38828
41. Ali A, Thompson CF, Balkovec JM, Graham DW, Hammond ML, Quraishi N, Tata JR, Einstein M, Ge L, Harris G, Kelly TM, Mazur P, Pandit S, Santoro J, Sitlani A, Wang C, Williamson J, Miller DK, Thompson CM, Zaller DM, Forrest MJ, Carballo-Jane E, Luell S 2004 Novel N-arylpyrazolo[3,2-c]-based ligands for the glucocorticoid receptor: receptor binding and in vivo activity. J Med Chem 47:2441–2452
42. Geller DS, Farhi A, Pinkerton N, Fradley M, Moritz M, Spitzer A, Meinke G, Tsai FT, Sigler PB, Lifton RP 2000 Activating mineralocorticoid receptor mutation in hypertension exacerbated by pregnancy. Science 289: 119–123
43. Dey R, Roychowdhury P, Mukherjee C 2001 Homology modelling of the ligand-binding domain of glucocorticoid receptor: binding site interactions with cortisol and corticosterone. Protein Eng 14:565–571
44. Lanz RB, Rusconi S 1994 A conserved carboxy-terminal subdomain is important for ligand interpretation and transactivation by nuclear receptors. Endocrinology 135: 2183–2195
45. Modarress KJ, Opoku J, Xu M, Sarlis NJ, Simons Jr SS 1997 Steroid-induced conformational changes at ends of the hormone-binding domain in the rat glucocorticoid receptor are independent of agonist versus antagonist activity. J Biol Chem 272:23986–23994
46. Warnmark A, Treuter E, Wright AP, Gustafsson JA 2003 Activation functions 1 and 2 of nuclear receptors: molecular strategies for transcriptional activation. Mol Endocrinol 17:1901–1909
47. Simons Jr SS, Sistare FD, Chakraborti PK 1989 Steroid binding activity is retained in a 16-kDa fragment of the steroid binding domain of rat glucocorticoid receptors. J Biol Chem 264:14493–14497
48. Segard-Maurel I, Jibard N, Schweizer-Groyer G, Cadepond F, Baulieu EE 1992 Mutations in the "zinc fingers" or in the N-terminal region of the DNA binding domain of the human glucocorticosteroid receptor facilitate its salt-induced transformation, but do not modify hormone binding. J Steroid Biochem Mol Biol 41:727–732
49. Xu M, Chakraborti PK, Garabedian MJ, Yamamoto KR, Simons SS 1996 Modular structure of glucocorticoid receptor domains is not equivalent to functional independence. Stability and activity of the steroid binding domain are controlled by sequences in separate domains. J Biol Chem 271:21430–21438
50. Picard D, Yamamoto KR 1987 Two signals mediate hormone-dependent nuclear localization of the glucocorticoid receptor. EMBO J 6:3333–3340
51. Pandit S, Geissler W, Harris G, Sitlani A 2002 Allosteric effects of dexamethasone and RU486 on glucocorticoid receptor-DNA interactions. J Biol Chem 277:1538–1543
52. Garside H, Stevens A, Farrow S, Normand C, Houle B, Berry A, Maschera B, Ray D 2004 Glucocorticoid Ligands Specify Different Interactions with NF-{κ}B by allosteric effects on the glucocorticoid receptor DNA binding domain. J Biol Chem 279:50050–50059
53. Kumar R, Baskakov IV, Srinivasan G, Bolen DW, Lee JC, Thompson EB 1999 Interdomain signaling in a two-domain fragment of the human glucocorticoid receptor. J Biol Chem 274:24737–24741
54. Ghali SA, Gottlieb B, Lumbroso R, Beitel LK, Elhaji Y, Wu J, Pinsky L, Trifiro MA 2003 The use of androgen receptor amino/carboxyl-terminal interaction assays to investigate androgen receptor gene mutations in subjects with varying degrees of androgen insensitivity. J Clin Endocrinol Metab 88:2185–2193
55. Kodama T, Shimizu N, Yoshikawa N, Makino Y, Ouchida R, Okamoto K, Hisada T, Nakamura H, Morimoto C, Tanaka H 2003 Role of the glucocorticoid receptor for regulation of hypoxia-dependent gene expression. J Biol Chem 278:33384–33391
56. Okamoto K, Tanaka H, Ogawa H, Makino Y, Eguchi H, Hayashi S, Yoshikawa N, Poellinger L, Umesono K, Makino I 1999 Redox-dependent regulation of nuclear import of the glucocorticoid receptor. J Biol Chem 274: 10363–10371
57. Miura T, Ouchida R, Yoshikawa N, Okamoto K, Makino Y, Nakamura T, Morimoto C, Makino I, Tanaka H 2001 Functional modulation of the glucocorticoid receptor and suppression of NF-κB-dependent transcription by ursodeoxycholic acid. J Biol Chem 276:47371–47378
58. Yamamoto K, Masuno H, Choi M, Nakashima K, Taga T, Ooizumi H, Umesono K, Sicinska W, VanHooke J, DeLuca HF, Yamada S 2000 Three-dimensional modeling of and ligand docking to vitamin D receptor ligand binding domain. Proc Natl Acad Sci USA 97:1467–1472
59. Choi M, Yamamoto K, Masuno H, Nakashima K, Taga T, Yamada S 2001 Ligand recognition by the vitamin D receptor. Bioorg Med Chem 9:1721–1730
60. Choi M, Yamamoto K, Itoh T, Makishima M, Mangelsdorf DJ, Moras D, DeLuca HF, Yamada S 2003 Interaction between vitamin D receptor and vitamin D ligands. Two-dimensional alanine scanning mutational analysis. Chem Biol 10:261–270
61. Roux S, Terouanne B, Couette B, Rafestin-Oblin ME, Nicolas JC 1999 Conformational change in the human glucocorticoid receptor induced by ligand binding is altered by mutation of isoleucine 747 by a threonine. J Biol Chem 274:10059–10065

Molecular Endocrinology **is published monthly by The Endocrine Society (http://www.endo-society.org), the foremost professional society serving the endocrine community.**

TRAIL-Transduced Dendritic Cells Protect Mice from Acute Graft-versus-Host Disease and Leukemia Relapse[1]

Katsuaki Sato,[2]* Takashi Nakaoka,[†] Naohide Yamashita,[†] Hideo Yagita,[§] Hiroshi Kawasaki,[‡] Chikao Morimoto,[‡] Masanori Baba,[¶] and Takami Matsuyama[||]

TRAIL preferentially induces apoptotic cell death in a wide variety of transformed cells, whereas it induces no apoptosis, but inhibits activation of Ag-specific T cells via blockade of cell cycle progression. Although accumulating results suggest that TRAIL is involved in the maintenance of immunological homeostasis under steady state conditions as well as in the initiation and progression of immunopathologies, the potential regulatory effect of TRAIL on immune responses and its therapeutic potential in immunological diseases remains unclear. We report in this study the potential usefulness of TRAIL-transduced dendritic cells (DCs) for the treatment of lethal acute graft-vs-host disease (GVHD) and leukemia relapse. DCs genetically modified to express TRAIL showed potent cytotoxicity against both alloreactive T cells and leukemic cells through the induction of apoptosis. In addition, treatment with genetically modified DCs expressing TRAIL of allogeneic BM transplants recipients with leukemia was effective for protection against acute GVHD and leukemia relapse. Thus, gene transfer of TRAIL to DCs is a novel modality for the treatment of acute GVHD and leukemia relapse by selective targeting of pathogenic T cells and leukemic cells. ***The Journal of Immunology*, 2005, 174: 4025–4033.**

Tumor necrosis factor-related apoptosis-inducing ligand, also known as Apo2 ligand, is a type II transmembrane protein belonging to the TNF family (1). TRAIL can potentially interact with five different receptors. These include death receptor (DR4[3]; TRAIL-R1), DR5 (TRAIL-R2), decoy receptor (DcR1; TRAIL-R3), DcR2 (TRAIL-R4), and a soluble receptor called osteoprotegerin (1). Receptors for TRAIL are constitutively expressed in a variety of cell types (1). In contrast, the constitutive expression of TRAIL was observed in liver NK cells, whereas the levels of TRAIL expression in T cells as well as NK cells can be markedly up-regulated after cell activation (2–5). In addition, TRAIL preferentially induces apoptotic cell death in a wide variety of transformed cells, whereas it induces no apoptosis, but inhibits activation of Ag-specific T cells via blockade of cell cycle progression (6, 7).

The presence of multiple receptors for TRAIL strongly suggests that TRAIL is involved in the maintenance of immunological homeostasis under steady state conditions as well as in the initiation and progression of immunopathologies. Previous studies have shown that TRAIL plays a crucial role in the surveillance of tumor initiation and metastasis in mice (2). Although the role of TRAIL in the negative selection of thymocytes remains controversial (8, 9), TRAIL plays a crucial role in the regulation of autoimmune diseases (6, 8, 10). However, the potential regulatory effect of TRAIL on immune responses and its therapeutic potential in immunological diseases are unknown.

Dendritic cells (DCs) are APC that consist of heterogeneous subsets with different lineages and maturity; they not only initiate immunity, but are also involved in the induction of tolerance in vivo (11–13). Therefore, in addition to their original application in the therapy of cancer and infectious diseases, strategies using immunoregulatory DCs are expected to be effective for the prevention and treatment of autoimmune diseases, allergic diseases, and allograft rejection.

Genetic modification of DCs with genes encoding immunoregulatory molecules provides a potential approach for Ag-specific regulation of T cell-mediated immunity by selectively targeting Ag-specific T cells. The use of these genetically modified DCs was reportedly effective for the prevention of experimental autoimmune and allergic diseases as well as allograft rejection in animals through the down-regulation of Ag-specific T cell responses (14–17).

Allogeneic bone marrow (BM) transplantation (BMT) is an effective treatment for hematologic malignancies as well as genetic disorders (18–21). However, acute graft-vs-host disease (GVHD), which is caused by alloreactive T cells in donor BM inocula, is a major cause of morbidity and mortality in patients undergoing allogeneic BMT (18–21). Although the incidence and severity of acute GVHD can be dramatically improved by T cell depletion or the combination of immunosuppressive agents, the risk of leukemia relapse may be increased in turn, possibly due to the lack of

---

*Laboratory for Dendritic Cell Immunobiology, Research Center for Allergy and Immunology, RIKEN Yokohama Institute, Yokohama, Japan; [†]Department of Advanced Medical Science, and [‡]Department of Clinical Immunology, Advanced Clinical Research Center, Institute of Medical Science, University of Tokyo, Tokyo, Japan; [§]Department of Immunology, Juntendo University School of Medicine, Tokyo, Japan; and [¶]Division of Antiviral Chemotherapy, Center for Chronic Viral Diseases, and [||]Department of Immunology, Field of Infection and Immunity, Graduate School of Medical and Dental Science, Kagoshima University, Kagoshima, Japan

Received for publication October 19, 2004. Accepted for publication January 16, 2005.

The costs of publication of this article were defrayed in part by the payment of page charges. This article must therefore be hereby marked *advertisement* in accordance with 18 U.S.C. Section 1734 solely to indicate this fact.

[1] This work was supported by grants from the Japan Rheumatism Foundation (to K.S.), the Uehara Memorial Foundation (to K.S.), and the Kanzawa Medical Research Foundation (to K.S.).

[2] Address correspondence and reprint requests to Dr. Katsuaki Sato, Laboratory for Dendritic Cell Immunobiology, Research Center for Allergy and Immunology, RIKEN Yokohama Institute, Suehiro-cho 1-7-22, Tsurumi, Yokohama, Kanagawa 230-0045 Japan. E-mail address: katsuaki@rcai.riken.jp

[3] Abbreviations used in this paper: DR, death receptor; Ad, adenovirus vector; BM, bone marrow; BMT, BM transplantation; DC, dendritic cell; DcR, decoy receptor; GVHD, acute graft-vs-host diseases; GVL, graft-vs-leukemia; hTRAIL, human TRAIL; iDC, immature DC; mDC, mature DC; MFI, mean fluorescence intensity; MNC, mononuclear cell; MOI, multiplicity of infection; mTRAIL, murine TRAIL; TBI, total body irradiation; TRAIL-Ad, Ad expressing TRAIL.

Copyright © 2005 by The American Association of Immunologists, Inc.

0022-1767/05/$02.00

antileukemia effect of allogeneic T cells infused, so-called graft-vs-leukemia (GVL) effect (19–21). Therefore, there is an increasing interest in the development of strategies that suppress acute GVHD but enhance the GVL effect.

In this study we report that genetically modified TRAIL-expressing DCs induce apoptotic cell death in alloreactive T cells and ameliorate acute GVHD while exerting an antileukemic effect.

Materials and Methods

Media and reagents

The medium used throughout was RPMI 1640 (Sigma-Aldrich) or DMEM (Sigma-Aldrich) supplemented with antibiotic-antimycotic (Invitrogen Life Technologies) and 10% heat inactivated FCS (Invitrogen Life Technologies). GM-CSF, IL-2, IL-4, IFN-γ, and soluble TRAIL were purchased from PeproTech.

Cell preparations

Human immature DCs (iDCs) were obtained by culturing peripheral blood monocytes with GM-CSF (50 ng/ml) and IL-4 (50 ng/ml) for 7 days (22). For the preparation of mature DCs (mDCs), cells were subsequently cultured with LPS (1 μg/ml; Sigma-Aldrich) for another 4 days (22). Murine iDCs were prepared by culturing BM cells obtained from female BALB/c mice (H-2^d) or C57BL/6 mice (H-2^b; all from Charles River Laboratories) with murine GM-CSF (20 ng/ml) for 8 days, and mDCs were obtained from culture of iDCs with LPS (1 μg/ml) for 4 days (21). Human T cells were purified from PBMC with a T cell negative isolation kit (Dynal Biotech), and $CD4^+$ T cells were then negatively selected from T cells with anti-CD8 mAb (BD Biosciences) plus goat anti-mouse IgG Ab-conjugated immunomagnetic beads (Dynal Biotech) (22). Murine T cells were negatively selected from splenic mononuclear cells (MNC) obtained from C57BL/6 mice with mAbs to Ly-76, B220, Ly-6G, and I-A/I-E (all from BD Biosciences) plus sheep anti-rat IgG Ab-conjugated immunomagnetic beads (Dynal Biotech) (21). Subsequently, $CD4^+$ T cells were negatively selected from T cells with anti-CD8 mAb (BD Biosciences) in combination with sheep anti-rat IgG Ab-conjugated immunomagnetic beads (21). Con A blasts were obtained from the culture of human or murine T cells with Con A (2.5 μg/ml; Sigma-Aldrich) for 3 days.

Production of adenovirus encoding the TRAIL genes

The full-length human TRAIL (hTRAIL) cDNA (884 bp) was prepared by RT-PCR amplification of total RNA from Con A blasts with the following oligonucleotide primers: 5′-CAG CAG TCA GAC TCT GAC AG-3′ and 5′-TCT TTC CAG GTC AGT TAG CC-3′. The PCR product was subcloned into pCR2.1 vector using TA Cloning kit (Invitrogen Life Technologies), and the nucleotide sequence was confirmed using a 373A automated sequencer (Applied Biosystems) and the fluoresceinated dye terminator cycle sequencing method. The full-length murine TRAIL (mTRAIL) cDNA was prepared from mTRAIL/pMKITNeo expression vector (23). After *Xho*I and *Not*I digestion, the 850 bp of mTRAIL cDNA was obtained, and the nucleotide sequence was confirmed as described above.

A replication-deficient adenovirus vector (Ad) expressed from the CAG promotor was generated using an Adenovirus Expression Vector kit (TaKaRa Shuzo), in which an adenoviral cosmid, pAxCAwt, was included. The cosmid pAxCAwt consisted of E1- and E3-deficient Ad type 5 (Ad5) sequences, and the CAG promoter and rabbit globin poly-A were inserted at the former E1 site in reverse orientation with respect to the Ad5 sequences. Briefly, the entire coding sequence of hTRAIL or mTRAIL was blunted using a DNA Blunting kit (TaKaRa Shuzo) and was then subcloned into the *Swa*I site of pAxCAwt. The resulting cosmids were named hTRAIL/pAxCAwt and mTRAIL/pAxCAwt, respectively. Transfection of human embryonic kidney 293 cells (RIKEN Cell Bank) with these cosmid vectors and Ad backbone sequences (DNA-TPC) that had the E1 and E3 genes deleted was performed according to the manufacturer's instructions to produce replication-incompetent, E1- and E3-deficient, Ad-expressing hTRAIL or mTRAIL (hTRAIL-Ad or mTRAIL-Ad). The viruses were then prepared by expansion of a single clone generated in 293 cells, which were purified by limiting dilution, and viral particles were isolated and amplified for analysis of hTRAIL or mTRAIL expression by flow cytometry. Recombinant adenoviruses generated from the homologous recombination of pAxCAwt and DNA-TPC were used as virus controls (control-Ad). Recombinant adenovirus titers were determined by plaque assays on 293 cells. These adenoviruses were suspended in culture medium, adjusted to 2×10^8 PFU/ml, and stored at −80°C until use.

Adenoviral infection

For Ad-mediated gene transfer into human DCs by centrifugal transduction (24), 500 μl of cells (10^6 cells) were mixed with 500 μl of adenoviral vector (multiplicity of infection (MOI) of 10 or 50), and 1 ml of the mixture was poured into a polypropylene tube (BD Biosciences). The tubes were centrifuged at $2000 \times g$ at 37°C for 2 h. After the centrifugal transduction, the cells were washed twice in PBS. DCs were resuspended in culture medium under various culture conditions and cultured for the indicated periods in tissue culture dishes (BD Biosciences). For adenoviral infection of murine DCs, 500 μl of iDCs (10^6 cells) were mixed with 500 μl of adenoviral vector (MOI of 50) in a polypropylene tube, and 1 ml of the mixture was incubated at 37°C. After a 2-h incubation, culture medium was added to the cells, then the cultures were incubated with LPS (1 μg/ml) for 4 days in tissue culture dishes.

Flow cytometry

Cells were stained with the following mAbs to human and murine markers: CD3, CD4, CD11c, CD40, CD80, CD86, HLA-A/B/C, HLA-DR, H-$2K^b$, H-$2K^d$, I-A/I-E, and isotype-matched control IgG (all from BD Biosciences); CD83 (Coulter Immunology); and FITC-conjugated goat anti-rat IgG Ab (Santa Cruz Biotechnology). The purified mAbs to hTRAIL (RIK-2), mTRAIL (N2B2), human DR4 (hDR4; DJR1), human DR5 (hDR5; DJR2), human DcR1 (hDcR1; DJR3), human DcR2 (hDcR2; DJR4), and murine DR5 (mDR5; MD5–1) were prepared as described previously (5, 25, 26). Fluorescent staining was analyzed on a FACScan flow cytometer using CellQuest software (BD Biosciences), and the data are expressed as the mean fluorescence intensity (MFI).

Cytotoxicity assay

Adenoviral gene-transduced untransduced DCs were cultured with $Na_2{}^{51}CrO_4$ (NEN Life Science Products)-labeled Jurkat cells, L929 cells, P815 cells (10^4; all from RIKEN Cell Bank), or Con A blasts (10^4) for 4 h at various E:T cell ratios in the presence or the absence of 10 μg/ml anti-hTRAIL mAb, anti-hDR5 mAb, anti-mTRAIL mAb, or control IgG. As a control, soluble hTRAIL was added to the target cells at the indicated concentrations (10–1000 ng/ml). The radioactivity of the supernatants was measured, and the percent-specific lysis was calculated (21, 22). Spontaneous release was <10% of total release.

Cell proliferation assay

Human $CD4^+$ T cells (10^5) were stimulated with or without plate-bound anti-human CD3 mAb (BD Biosciences) plus soluble anti-human CD28 mAb (BD Biosciences) in the presence or the absence of soluble hTRAIL (1000 ng/ml), anti-hTRAIL mAb, or control Ig (each 10 μg/ml). For human and murine allogeneic MLR, $CD4^+$ T cells (10^5) were cultured in 96-well plates (BD Biosciences) with various numbers of irradiated (15 Gy from a ^{137}Cs source; MBR-1505R2; Hitachi Medical) allogeneic DCs in the presence or the absence of soluble hTRAIL (1000 ng/ml), anti-hTRAIL mAb (10 μg/ml), anti-mTRAIL mAb (10 μg/ml), anti-hDR5 mAb (10 μg/ml), or control Ig (10 μg/ml). [^{3}H]Thymidine incorporation was measured on day 5 for the last 18 h (21, 22).

In vitro analysis of T cell responses

For measuring cell division, $CD4^+$ T cells were labeled with CFSE (Molecular Probes) according to the manufacturer's instructions. CFSE-labeled $CD4^+$ T cells (5×10^6) were cultured with irradiated (15 Gy) allogeneic DCs (5×10^5) for 3 days, then T cells were negatively selected with anti-human CD11c mAb (BD Biosciences) plus goat anti-mouse IgG Ab-conjugated immunomagnetic beads (22). These T cell preparations contained <0.1% $CD11c^+$ cells as assessed by FACS analysis. The CFSE-positive cells were then analyzed by flow cytometry. Apoptosis in allogeneic DC-stimulated $CD4^+$ T cells was measured by flow cytometry using an Annexin V^{FITC} apoptosis detection kit (R&D Systems). For cell cycle analysis, the stimulated $CD4^+$ T cells were incubated with BrdU (BD Biosciences) at 10 μM for 1 h at 37°C. Staining of incorporated BrdU was performed using a BrdU Flow kit (BD Bioscience) according to the manufacturer's instructions. Cells were stained with FITC-conjugated anti-BrdU Ab for 20 min at room temperature. 7-Amino-actinomycin D (20 μg/ml) was added to the cell suspension before flow cytometric analysis.

Acute GVHD model

BALB/c recipient mice (five animals in each group) received lethal total body irradiation (TBI; 10 Gy) and then a single i.v. injection of C57BL/6 BM cells (1.5×10^7/mouse) plus splenic MNC (1.5×10^7/mouse) through the tail vein (21). The day of transplantation was designated day 0. The i.v.

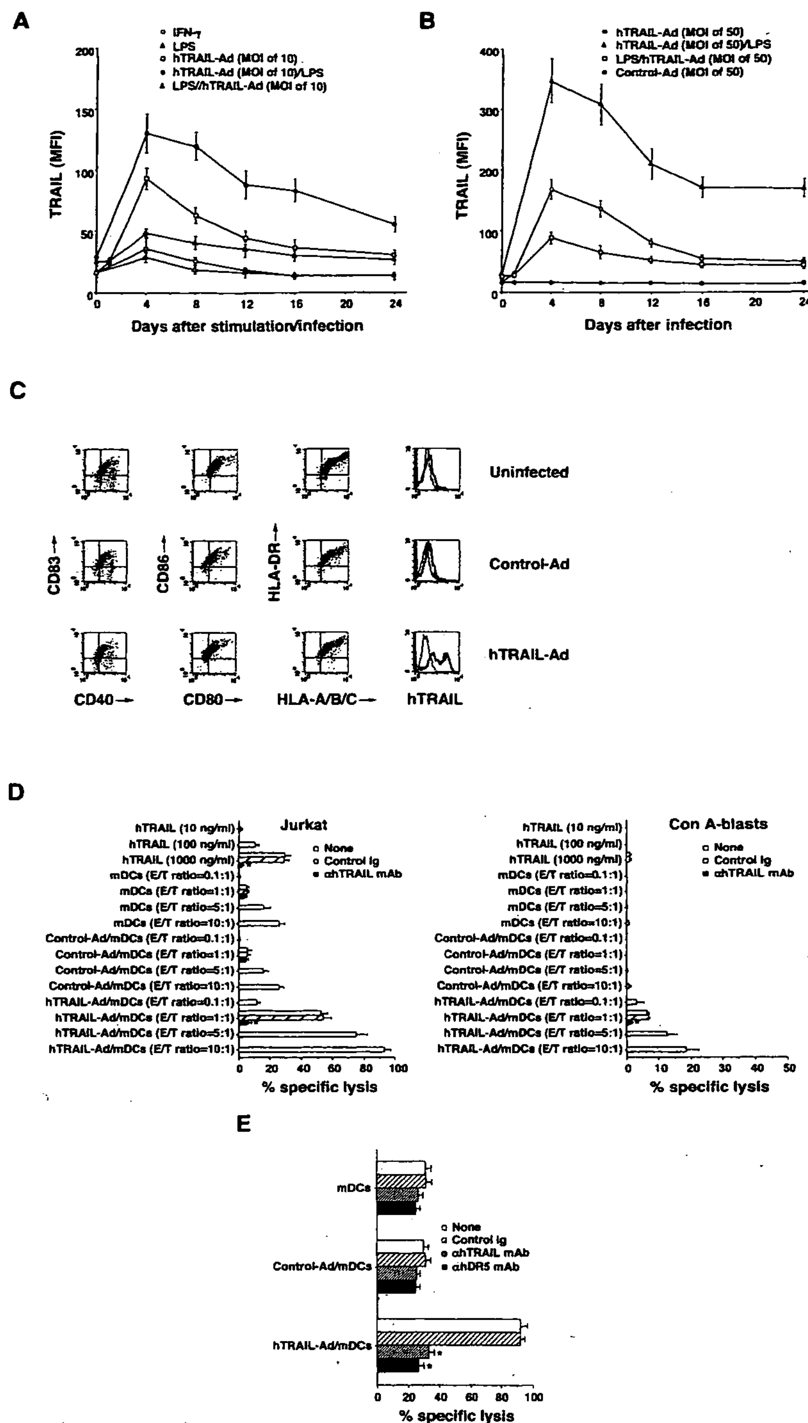

FIGURE 1. Generation of genetically modified human DCs expressing TRAIL. *A* and *B*, The iDCs were not infected or were infected with control-Ad or hTRAIL-Ad at MOI of 10 (*A*) and 50 (*B*). In some experiments, uninfected DCs or DCs infected with hTRAIL-Ad were stimulated with IFN-γ (*A*) or LPS (*A* and *B*) before or after infection. The expression of hTRAIL on DCs was analyzed by flow cytometry at the indicated time points. The expression level of TRAIL was expressed as the mean MFI ± SD of four individual experiments. The results are representative of two experiments with similar results. *C*, The iDCs were not infected or were infected with control-Ad or hTRAIL-Ad at an MOI of 50, followed by stimulation with LPS for generation of mDCs. Subsequently, mDCs were stained with the indicated mAbs, and cell surface expression was analyzed by flow cytometry. Data are represented by a dot plot for the expression of MHC and costimulatory molecules or by a histogram in which cells were stained with anti-hTRAIL mAb (thick lines) or isotype-matched control Ig (thin lines). The results are representative of four experiments with similar results. *D*, The cytotoxicity of soluble hTRAIL, uninfected DCs, or DCs infected with control-Ad or hTRAIL-Ad against Jurkat cells or Con A blasts at various E:T cell ratios in the presence or the absence of control Ig or anti-hTRAIL mAb was analyzed by the 4-h ^{51}Cr release assay. Data were expressed as the mean ± SD of triplicate samples, and the results are representative of four experiments with similar results. *E*, The cytotoxicity of soluble hTRAIL, uninfected DCs, or DCs infected with control-Ad or hTRAIL-Ad against Jurkat cells at an E:T cell ratio of 10 in the presence or the absence of control Ig, anti-hTRAIL mAb, or anti-hDR5 mAb was analyzed by the 4-h ^{51}Cr release assay. Data were expressed as the mean ± SD of triplicate samples, and the values shown are representative of four experiments with similar results. *, $p < 0.01$ compared with control Ig, by Student's paired *t* test.

injection of adenoviral gene-transduced or untransduced DCs from BALB/c mice or C57BL/6 mice (10^6 to 5×10^6/mouse) 2 days after transplantation. For the in vivo blockade experiments, recipients were i.p. injected with control Ig or anti-mTRAIL mAb (1 mg/mouse) before i.v. injection of DCs. The recipients were monitored every day for survival. Some recipients were killed 5 days after transplantation to obtain serum and splenic MNCs.

Leukemia relapse model

BALB/c recipients (five animals in each group) were inoculated i.v. with P815 cells (2×10^5/mouse) 2 days before TBI (10 Gy) and i.v. transplantation with C57BL/6 BM cells (1.5×10^7/mouse) (21). The transplanted recipients received a single i.v. injection of adenoviral gene-transduced or untransduced DCs from BALB/c mice (5×10^6/mouse) 2 days after transplantation. Recipients were monitored every day for survival. Hepatosplenomegaly due to tumor burden in the dead mice was confirmed by laboratory.

Statistical analyses

Statistically significant differences were determined by Student's paired *t* test or Mann-Whitney's *U* test. A value of $p < 0.01$ was considered significant.

Results

Regulatory function of human DCs genetically modified to express TRAIL

To test the potential use of TRAIL-expressing DCs for selectively targeting Ag-specific T cells, we examined the conditions for the

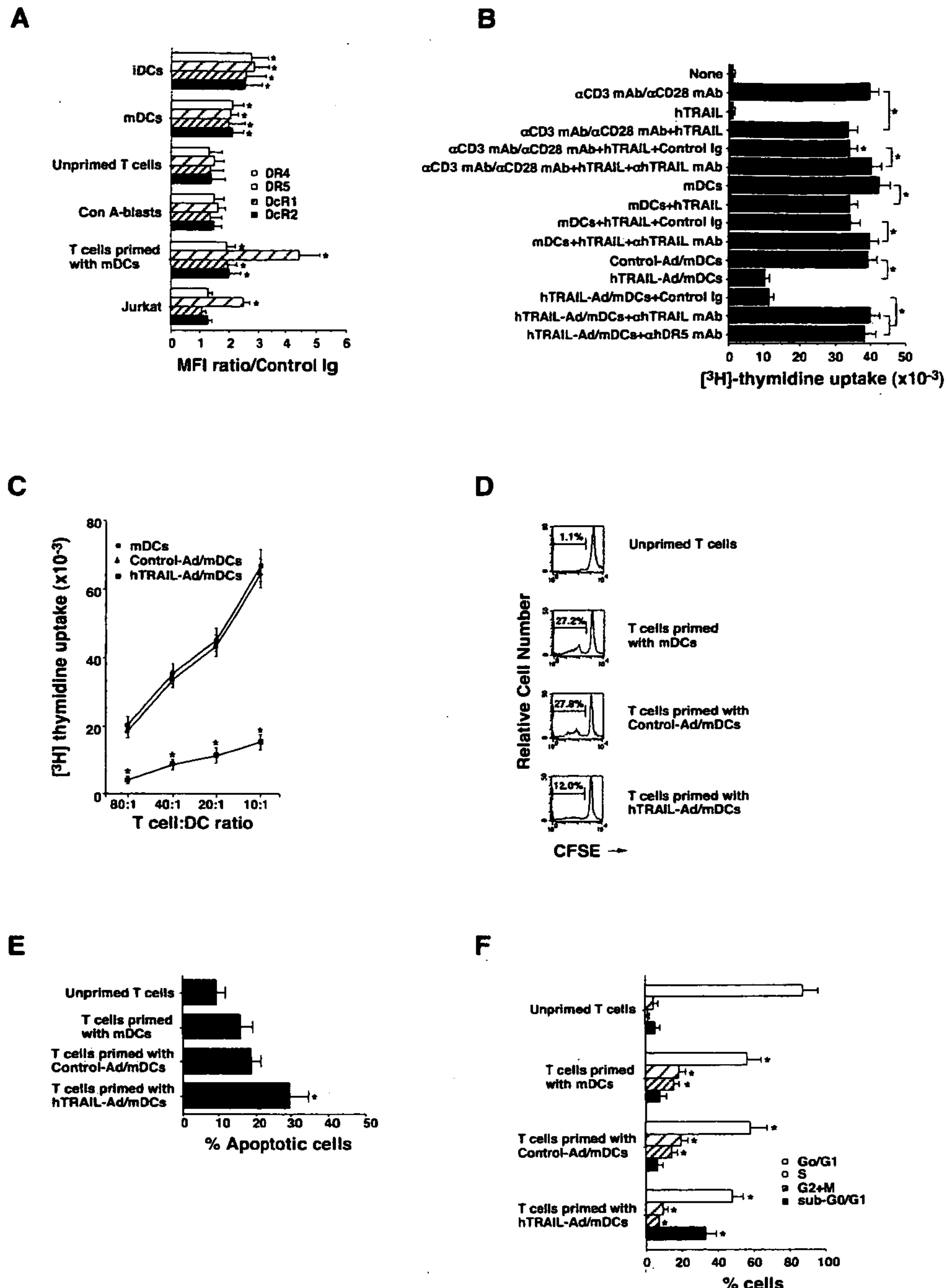

FIGURE 2. Regulatory function of human DCs genetically modified to express TRAIL. *A*, The expression of TRAIL receptors on the indicated cells was analyzed by flow cytometry. Values were expressed as the ratio of MFI with respective mAb compared with the MFI with control Ig, and data are expressed as the mean ± SD of four individual experiments. *, $p < 0.01$ compared with control Ig, by Student's paired *t* test. *B*, Human $CD4^+$ T cells (10^5) were stimulated with or without plate-bound anti-human CD3 plus soluble anti-human CD28 mAb in the presence or the absence of soluble hTRAIL and anti-hTRAIL mAb or control Ig. In another experiment, $CD4^+$ T cells (10^5) were cultured with uninfected or control-Ad or hTRAIL-Ad-infected allogeneic mDCs (10^4) in the presence or the absence of soluble hTRAIL, anti-hTRAIL mAb, anti-hDR5 mAb, or control Ig. The proliferative response was measured by [^{3}H]thymidine uptake on day 5. Data were expressed as the mean ± SD of triplicate samples, and the values shown are representative of four experiments with similar results. *, $p < 0.01$, by Student's paired *t* test. *C*, $CD4^+$ T cells (10^5) were cultured with various numbers of uninfected or control-Ad- or hTRAIL-Ad-infected allogeneic mDCs, and the proliferative response was measured by [^{3}H]thymidine uptake on day 5. Data were expressed as the mean ± SD of triplicate samples, and the values shown are representative of four experiments with similar results. *, $p < 0.01$ compared with uninfected DCs, by Student's paired *t* test. *D*, CFSE-labeled $CD4^+$ T cells (5×10^6) were primed with uninfected or control-Ad- or hTRAIL-Ad-infected allogeneic mDCs (5×10^5) for 3 days, and CFSE levels were analyzed by flow cytometry. Data are represented by a histogram. The data shown are representative of four experiments with similar results. *E* and *F*, $CD4^+$ T cells (5×10^6) were primed with uninfected or control-Ad- or hTRAIL-Ad-infected allogeneic mDCs (5×10^5) for 3 days, then $CD4^+$ T cells were analyzed for apoptosis (*E*) or cell cycle (*F*) by flow cytometry. Data were expressed as the mean ± SD of triplicate samples, and the values shown are representative of four experiments with similar results. *, $p < 0.01$ compared with T cells primed with mDCs (*E*) or unprimed T cells (*F*), by Student's paired *t* test.

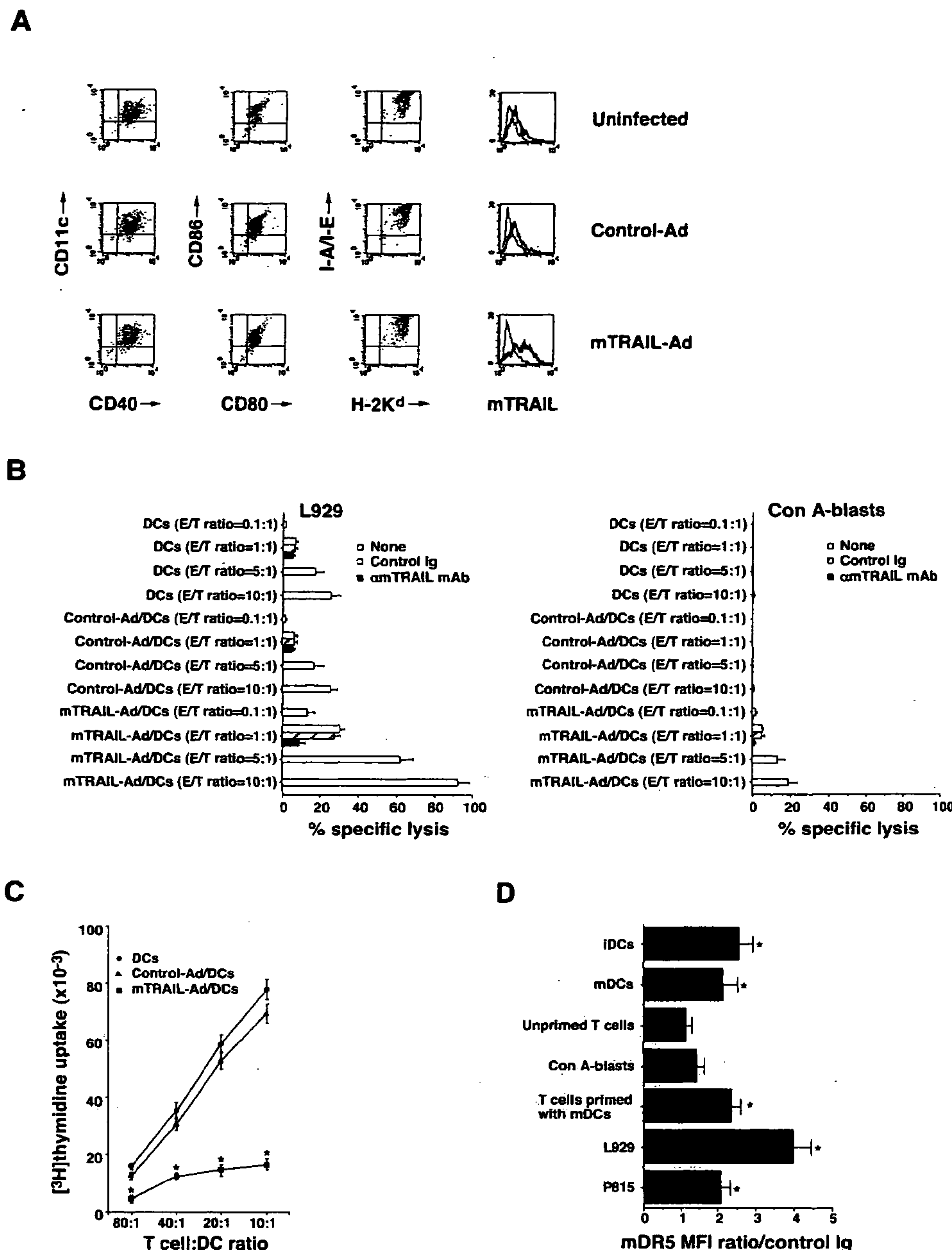

FIGURE 3. Regulatory function of murine DCs genetically modified to express TRAIL. *A*, Murine DCs were uninfected or infected with control-Ad or mTRAIL-Ad at an MOI of 50, followed by stimulation with LPS. Subsequently, DCs were stained with the indicated mAbs, and cell surface expression was analyzed by flow cytometry. Data are represented by a dot plot for the expression of MHC and costimulatory molecules or by a histogram in which cells were stained with anti-hTRAIL mAb (thick lines) or isotype-matched control Ig (thin lines). The data shown are representative of four experiments with similar results. *B*, The cytotoxicity of uninfected DCs or DCs infected with control-Ad or mTRAIL-Ad against L929 cells or Con A blasts was analyzed in the presence or the absence of control Ig or anti-mTRAIL mAb. Data were expressed as the mean ± SD of triplicate samples, and the values shown are representative of four experiments with similar results. *C*, $CD4^+$ T cells (10^5) from naive C57BL/6 mice were cultured with various numbers of uninfected or control-Ad- or mTRAIL-Ad-infected mDCs from BALB/c mice, and the proliferative response was measured on day 5 by [^{3}H]thymidine uptake. Data were expressed as the mean ± SD of triplicate samples, and the values shown are representative of four experiments with similar results. *, $p < 0.01$ compared with uninfected DCs, by Student's paired *t* test. *D*, The expression of DR5 on the indicated murine cells was analyzed by flow cytometry. Values were expressed as the ratio of MFI with anti-DR5 mAb compared with the MFI with control Ig, and data are expressed as the mean ± SD of four individual experiments. *, $p < 0.01$ compared with control Ig, by Student's paired *t* test.

generation of human DCs genetically engineered to express TRAIL using Ad. Although stimulation of iDCs with IFN-γ or LPS induced low levels of TRAIL expression (27, 28), adenoviral gene transduction of hTRAIL (hTRAIL-Ad) into DCs resulted in higher expression of TRAIL. Of note, introduction of hTRAIL-Ad into iDCs followed by stimulation with LPS (Fig. 1, *A* and *B*) or TNF-α (data not shown) resulted in the generation of mDCs with the highest level of TRAIL expression. Adenoviral infection had little or no effect on the expression of MHC and costimulatory molecules (Fig. 1*C*). The hTRAIL-Ad-infected mDCs (hTRAIL-Ad/mDCs) showed a more potent killing activity against hTRAIL-sensitive Jurkat cells than soluble hTRAIL, mDCs, and control-Ad-infected mDCs (control-Ad/mDCs; Fig. 1*D*). In addition, the cytotoxicity of hTRAIL-Ad/mDCs against Jurkat cells was blocked by anti-hTRAIL mAb and anti-hDR5 mAb (Fig. 1, *D* and *E*). These results indicate that hTRAIL was functionally expressed on the hTRAIL-Ad/mDCs. In contrast, Con A blasts (Fig. 1*C*) and DCs (data not shown) were relatively resistant to TRAIL-mediated cytotoxicity.

We also examined the expression levels of TRAIL receptors on various cell types (Fig. 2*A*). The iDCs constitutively expressed DR4, DR5, DcR1, and DcR2 at similar levels, and the expression of these receptors was slightly reduced after maturation. Unlike Jurkat cells, which predominantly expressed DR5, little or no expression of these receptors was observed on unstimulated $CD4^+$ T cells and Con A blasts. Interestingly, stimulation of $CD4^+$ T cells with allogeneic mDCs induced specific up-regulation of DR5, whereas stimulation with anti-CD3 and anti-CD28 mAbs up-regulated DR5 to a lesser degree (data not shown).

We also examined the T cell regulatory function of hTRAIL-Ad/DCs. Soluble TRAIL showed a minimal inhibition of proliferation when $CD4^+$ T cells were stimulated with anti-CD3 and anti-CD28 mAbs or allogeneic mDCs (Fig. 2*B*). In contrast, hTRAIL-Ad/DCs, but not control-Ad/mDCs, displayed a potent suppressive effect on the proliferation of alloreactive $CD4^+$ T cells (Fig. 2, *B* and *C*). This suppression was abrogated by both anti-hTRAIL mAb and anti-hDR5 mAb, but not by control Ig (Fig. 2*B*). These results indicate that DCs genetically modified to express

TRAIL could inhibit the proliferation of allogeneic CD4$^+$ T cells through the interaction with DR5.

Previous studies have shown that soluble TRAIL did not induce apoptosis, but inhibited the proliferation of T cells through blockage of cell cycle progression (6, 7). To clarify the mechanism underlying the T cell regulatory function of TRAIL-transduced DCs, we characterized CD4$^+$ T cells primed with hTRAIL-Ad/DCs. The CFSE labeling assay showed that the proportion of dividing cells was significantly reduced in allogeneic CD4$^+$ T cells primed with hTRAIL-Ad/DCs compared with those primed with mDCs and control-Ad/mDCs (Fig. 2*D*). In contrast, hTRAIL-Ad/DCs induced significantly more apoptosis in allogeneic CD4$^+$ T cells than mDCs and control-Ad/mDCs (Fig. 2*E*). Also in the cell cycle analysis, numerous apoptotic cells with sub-G_0/G_1 DNA content were detected in allogeneic CD4$^+$ T cells primed with hTRAIL-Ad/DCs, whereas the proliferating cells in S phase and G_2+M phase were increased in allogeneic CD4$^+$ T cells primed with mDCs or control-Ad/mDCs (Fig. 2*F*). These results indicate that the DCs genetically modified to express TRAIL suppress the proliferation and cell division of allogeneic CD4$^+$ T cells through the induction of apoptosis rather than cell cycle arrest.

TRAIL-transduced DCs ameliorate murine acute GVHD

The above results indicated that mDCs genetically modified to express hTRAIL could efficiently suppress the proliferation of alloreactive CD4$^+$ T cells through the induction of apoptosis. We therefore tested the in vivo suppressive function of murine DCs genetically modified to express mouse TRAIL (mTRAIL-Ad/DCs). Similar to hTRAIL-Ad/mDCs, mTRAIL-Ad/DCs showed the functional expression of mTRAIL (Fig. 3, *A* and *B*). In addition, mTRAIL-Ad/DCs impaired the proliferation of alloreactive CD4$^+$ T cells (Fig. 3*C*), and they induced a higher rate of apoptosis in allogeneic CD4$^+$ T cells than control-Ad/DCs (data not shown).

We also examined the expression level of mDR5 on various cell types (Fig. 3*D*). Flow cytometric analysis showed that mTRAIL-sensitive L929 cells as well as P815 cells expressed high level of mDR5. In contrast, mDCs exhibited slightly lower expression of mDR5 than mDCs. We also observed that DCs expressed the transcripts of all TRAIL receptors at similar levels, and these transcriptional expressions were reduced after maturation (data not shown). In addition, the primed CD4$^+$ T cells with allogeneic mDCs showed higher expression of mDR5 than unstimulated CD4$^+$ T cells and Con A blasts.

We then tested the therapeutic efficacy of mTRAIL-Ad/DCs against acute GVHD. All BALB/c recipients died on day 8 after transplantation of C57BL/6 BM and spleen cells (Fig. 4*A*). In these mice, clinical symptoms of acute GVHD, such as hair ruffling, lower mobility, and weight loss, became apparent within 6 days. In contrast, all BALB/c recipients of syngeneic BM and spleen cells survived >60 days without apparent acute GVHD (data not shown). A single injection of BALB/c-derived DCs or control-Ad/DCs 2 days after transplantation of C57BL6 BM and spleen cells to BALB/c recipients did not significantly affect the lethality caused by acute GVHD (Fig. 4*A*). In contrast, BALB/c-derived mTRAIL-Ad/DCs ameliorated acute GVHD in a dose-dependent fashion (Fig. 4*A*), whereas C57BL/6-derived mTRAIL-Ad/DCs showed a minimal inhibitory effect (Fig. 4*B*). In addition, in vivo blockade of mTRAIL with anti-mTRAIL mAb abrogated the therapeutic effect of mTRAIL-Ad/DCs (Fig. 4*C*).

We also examined the in vivo regulatory effect of mTRAIL-Ad/DCs in the recipients of allogeneic transplantation. The administration of mTRAIL-Ad/DCs significantly reduced the number of total splenocytes (Fig. 5*A*) and inhibited the expansion of donor-derived CD4$^+$ and CD8$^+$ T cells in the spleen (Fig. 5*B*), whereas that of untransduced DCs increased the number of these cells. Moreover, donor-derived CD4$^+$ T cells from the mTRAIL-Ad/DC-treated recipients showed a significantly reduced proliferative

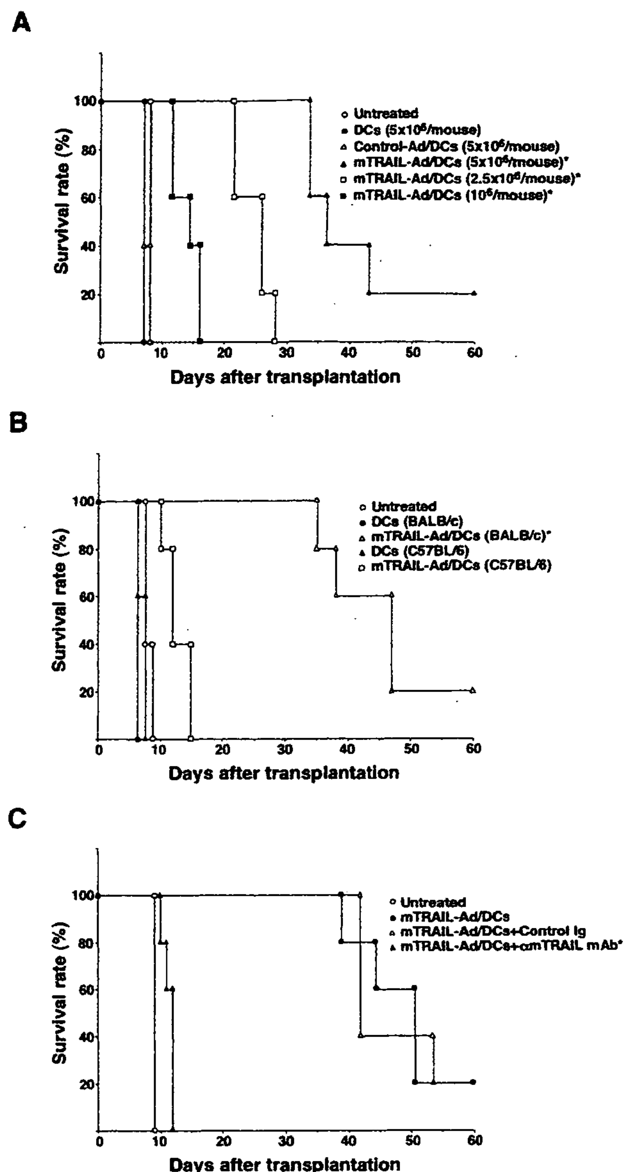

FIGURE 4. Suppressive effect of TRAIL-transduced murine DCs on acute GVHD in murine allogeneic BMT. *A*, BALC/c recipient mice of C57BL/6 BMT were i.v. injected with or without uninfected or control-Ad- or mTRAIL-Ad-infected BALB/c DCs (10^6 to 5×10^6/mouse) on 2 days after BMT. Mice were monitored daily for survival. The results are representative of two individual experiments with similar results. *, $p < 0.01$ compared with untreated mice, by Mann-Whitney's *U* test. *B*, BALC/c recipient mice of C57BL/6 BMT were i.v. injected with or without uninfected or mTRAIL-Ad-infected BALB/c or C57BL/6 DCs (5×10^6/mouse) on 2 days after BMT. Mice were monitored daily for survival. The results are representative of two individual experiments with similar results. *, $p < 0.01$ compared with untreated mice, by Mann-Whitney's *U* test. *C*, BALC/c recipient mice of C57BL/6 BMT were i.v. injected with or without mTRAIL-Ad-infected BALB/c DCs (5×10^6/mouse) and control Ig or anti-mTRAIL mAb on 2 days after BMT. Mice were monitored daily for survival. The results are representative of two individual experiments with similar results. *, $p < 0.01$ compared with control Ig-treated mice, by Mann-Whitney's *U* test.

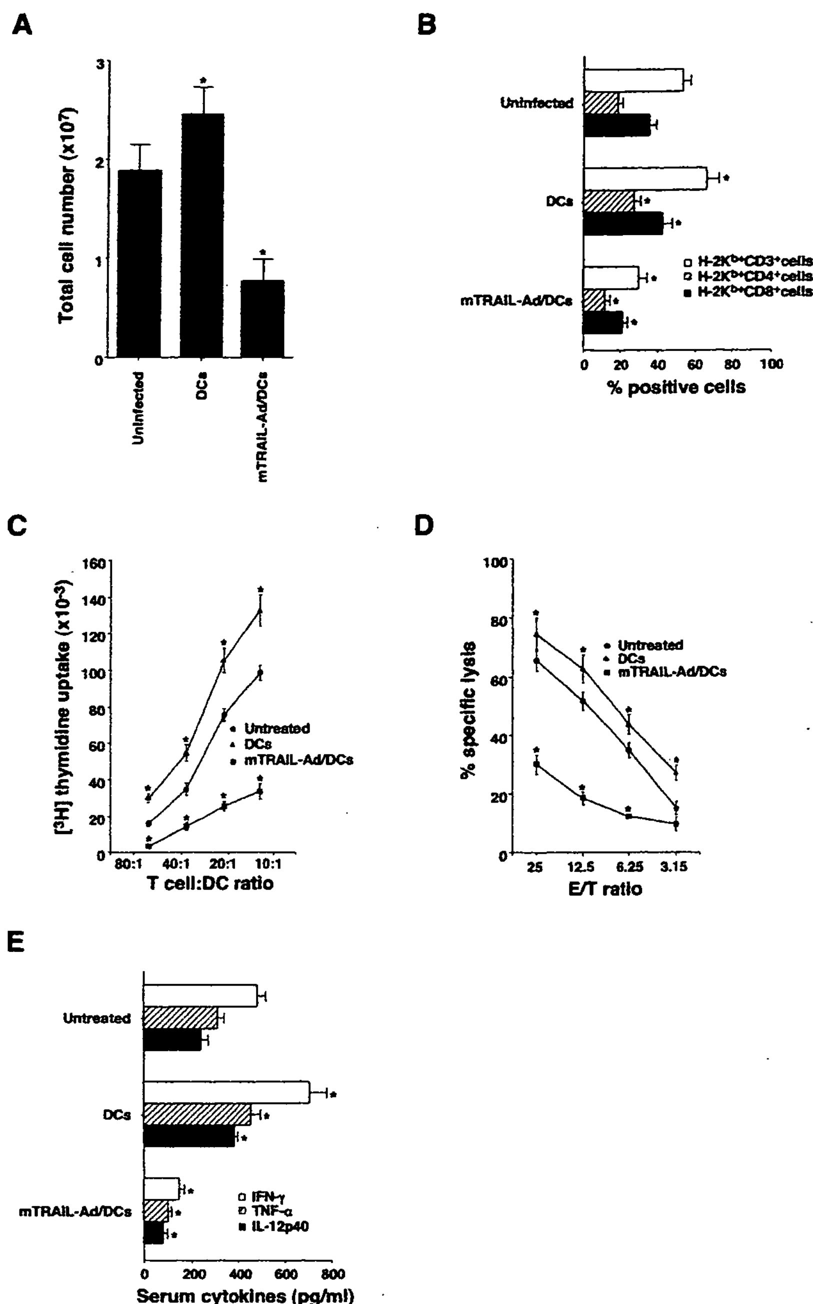

FIGURE 5. Suppressive effect of TRAIL-transduced murine DCs on allogeneic responses of donor-derived T cells in transplanted mice. *A–E*, BALC/c recipient mice of C57BL/6 BMT were i.v. injected with or without uninfected or mTRAIL-Ad-infected BALB/c DCs (5 × 10^6/mouse) on 2 days after BMT. On 5 days after BMT, splenic MNC and sera were obtained from indicated mice. *A*, The number of donor-derived (H-2^{b+}) splenic MNC was analyzed by flow cytometry. Data were expressed as the mean ± SD of five mice in each group. *, $p < 0.01$ compared with untreated recipients, by Student's paired *t* test. *B*, The constitution of donor-derived (H-2^{b+}) T cell subsets was analyzed by flow cytometry. Data are expressed as the mean ± SD of five mice in each group. *, $p < 0.01$ compared with untreated recipients, by Student's paired *t* test. *C*, Donor-derived $CD4^+$ T cells (10^5) were cultured with various numbers of irradiated BALB/c DCs, and the proliferative response was measured by [^{3}H]thymidine uptake on day 5. Data were expressed as the mean ± SD of triplicate samples, and the values shown are representative of four experiments with similar results. *, $p < 0.01$ compared with untreated recipients, by Student's paired *t* test. *D*, Donor-derived $CD8^+$ T cells were subjected to CTL assay against P815 cells at various E:T cell ratios. Data were expressed as the mean ± SD of triplicate samples, and the values shown are representative of four experiments with similar results. *, $p < 0.01$ compared with untreated recipients, by Student's paired *t* test. *E*, Concentrations of IFN-γ, TNF-α, and IL-12p40 in serum were evaluated by ELISA. Data are expressed as the mean ± SD of five mice in each group. *, $p < 0.01$ compared with untreated recipients, by Student's paired *t* test.

response to the host-type mDCs, whereas those from the DC-treated recipients showed an enhanced response (Fig. 5*C*). Furthermore, donor-derived $CD8^+$ T cells from the mTRAIL-Ad/DC-treated recipients showed markedly impaired CTL activity against P815 cells expressing the host-type alloantigen, whereas those from the DC-treated recipients showed enhanced CTL activity (Fig. 5*D*). In addition, mTRAIL-Ad/DC-treated recipients showed a significant reduction of production of serum IFN-γ, TNF-α, and IL-12p40 compared with untreated and control-Ad/DC-treated recipients (Fig. 5*E*). These results indicate that mTRAIL-Ad/DCs is could efficiently ameliorate acute GVHD through the suppression of alloreactive T cell responses.

Protection from leukemia relapse by mTRAIL-transduced DCs

TRAIL has been implicated in the GVL effect associated with allogeneic BMT (20). Therefore, we next examined the antileukemic effect of TRAIL-transduced DCs. The recipient mice were i.v. inoculated with or without P815 leukemia cells 2 days before TBI and transplantation of allogeneic BM cells. Consistent with previous reports (20, 21), the mice transplanted with allogeneic BM cells alone survived >60 days without apparent acute GVHD. All leukemia-bearing mice that received TBI alone died within 14 days with marked hepatosplenomegaly. In contrast, the leukemia-bearing recipients of allogeneic BM cells died within 26 days after transplantation, indicating that alloreactive T cells in BM cells exhibited an insufficient GVL effect. We then examined the therapeutic effect of mTRAIL-transduced DCs against leukemia relapse in this model. The mTRAIL-Ad/DCs showed potent cytotoxicity against P815 cells in vitro (Fig. 6*A*). A single injection of recipient-type mTRAIL-Ad/DCs, but not DCs or control-Ad/DCs, 2 days after transplantation markedly prolonged the survival of leukemia-bearing mice (Fig. 6*B*). These results suggested that TRAIL-transduced DCs are useful not only to ameliorate acute GVHD but also to suppress leukemia relapse.

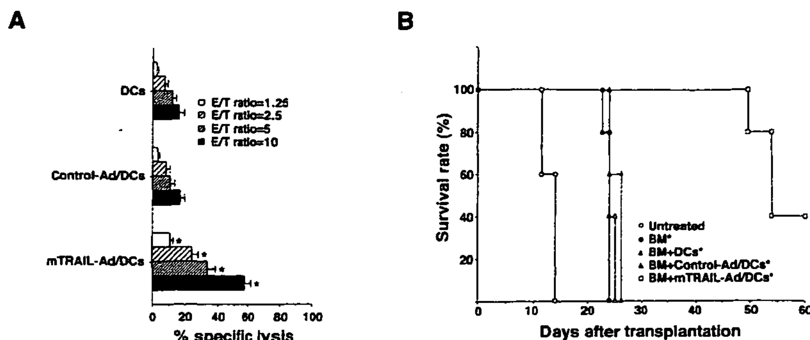

FIGURE 6. Protective effect of TRAIL-transduced murine DCs against leukemia relapse. *A*, The cytotoxicity of uninfected or control-Ad- or mTRAIL-Ad-infected DCs against P815 cells was analyzed by the 4-h ^{51}Cr release assay. Data were expressed as the mean ± SD of triplicate samples, and the values shown are representative of four experiments with similar results. *, $p < 0.01$ compared with uninfected DCs, by Student's paired *t* test. *B*, BALB/c recipient mice were inoculated i.v. with P815 cells (2×10^5) on day −2 and received TBI and i.v. transplantation with C57BL/6 BM cells on day 0. The recipient mice were i.v. injected with or without uninfected or control-Ad- or mTRAIL-Ad-infected BALB/c DCs (5×10^6/mouse) on day 2. Mice were monitored daily for survival. The results are representative of two individual experiments with similar results. *, $p < 0.01$ compared with untreated mice, by Mann-Whitney's *U* test.

Discussion

Gene transfer of immunoregulatory molecules to Ag-presenting DCs provides an attractive approach for the treatment of immunological diseases. Our present findings demonstrate the efficacy of TRAIL gene-transduced DCs for the therapy of lethal acute GVHD and leukemia relapse via elimination of the pathogenic T cells and leukemia cells.

Efficient expression of the introduced gene in target cells is crucial for regulating their function. We showed that the gene transfer of TRAIL into iDCs followed by inflammatory stimulation caused maximal expression of TRAIL. The precise molecular mechanism by which inflammatory stimulation up-regulated the expression of transduced TRAIL gene in DCs remains unknown, but inflammatory stimulation might activate certain transcriptional factors, leading to transactivation of the transduced TRAIL gene. In contrast, mDCs show more potent interaction with Ag-specific T cells than iDCs due to their higher expression of MHC and adhesion/costimulatory molecules. Thus, the maturation of iDCs genetically engineered to express TRAIL by inflammatory stimulation provides advantages for TRAIL expression as well as Ag-specific interaction with T cells.

We showed that human and murine TRAIL-sensitive cell types, including $CD4^+$ T cells primed with allogeneic DCs as well as Jurkat cells and L929 cells, exhibited high expression of DR5, indicating that DR5 is crucial for TRAIL-mediated cytotoxicity. In contrast, analysis of the cell surface expression of TRAIL receptors as well as their transcriptional expression (data not shown) revealed that human and murine DCs showed similar expression levels of these TRAIL receptors. Therefore, suppression of binding of TRAIL to DRs by DcRs may contribute to the low sensitivity of these cell types to TRAIL-mediated cytotoxicity. Collectively, our results suggest that the balance of the expression of DRs and DcRs may determine the sensitivity to TRAIL-mediated cytotoxicity.

The weak suppressive effect of recombinant soluble TRAIL on alloreactive T cell proliferation might be due to a blockage of cell cycle progression as previously reported (6, 7), whereas mDCs genetically modified to express TRAIL could effectively induce apoptosis in alloreactive T cells. Although the precise molecular mechanism underling the difference in the biological function between soluble TRAIL and membrane-bound transduced TRAIL on DCs remains unknown, this phenomenon might reflect the strength of intracellular signaling via DRs. Additional study will be needed to test this possibility.

Although host-matched or -mismatched mTRAIL-transduced DCs may lyse donor-derived T cells that overexpresses mDRs regardless of histocompatibility differences, host-matched mTRAIL-transduced DCs could more effectively lyse host-reactive, donor-derived T cells than host-mismatched, mTRAIL-transduced DCs, because they show more potent reactivity to host-matched, mTRAIL-transduced DCs than host-mismatched, mTRAIL-transduced DCs. Indeed, BALB/c-derived, mTRAIL-Ad/DCs, but not C57BL/6-derived, mTRAIL-Ad/DCs, ameliorated acute GVHD in BALB/c recipients transplanted with C57BL6 BM and spleen cells. Therefore, host-type, TRAIL-transduced DCs are useful for the protection of recipients from lethality induced by acute GVHD in allogeneic BMT.

The expansion of donor-derived $CD4^+$ and $CD8^+$ T cells was markedly suppressed by a single injection of host-type, mTRAIL-transduced DCs. These results suggest that interaction of alloreactive $CD4^+$ and $CD8^+$ T cells with the infused TRAIL-transduced mDCs caused their apoptosis via up-regulation of mDR5, resulting in their selective elimination in vivo. In contrast, donor-derived $CD4^+$ T cells obtained from these protected recipients showed a reduced proliferative response to host-type mDCs. Our results imply that the intracellular signaling events involving TRAIL/DR5 induce not only apoptosis but also functional deficiency in the targeted $CD4^+$ T cells. We also showed that the CTL activity of donor-derived $CD8^+$ T cells was greatly impaired in these protected recipients. Although the precise mechanism remains unclear, the functional impairment of donor-derived $CD4^+$ T cells may contribute to the reduced response of donor-derived $CD8^+$ T cells.

The deletion of donor-derived alloreactive T cells by mTRAIL-transduced DCs can ameliorate acute GVHD, but also may impair their GVL effect. However, our results showed that the TRAIL-transduced DCs could protect BMT recipients from leukemia relapse. This seems likely to be mediated by antileukemic effect of TRAIL expressed on DCs, because the TRAIL-transduced DCs exhibited potent cytotoxic activity in vitro. The ex vivo removal of donor T cell proportions from the marrow graft not only reduced the incidence and severity of acute GVHD, but also increased the risk of leukemia relapse due to lack of GVL effect (19–21). Therefore, our results imply that the use of TRAIL-transduced DCs and T cell-depleted BM inocula might be an alternative strategy for the prevention of acute GVHD and leukemia relapse in human leukemia patients undergoing allogeneic BMT.

The role of TRAIL in hepatic cell death is controversial (29, 30). We observed that a single injection of mTRAIL-Ad/DCs did not induce any apparent liver cytotoxicity in normal mice or recipients of allogeneic BMT (data not shown). Additional study will be needed to determine the safety and potential side effects of TRAIL-transduced DCs in vivo.

In the present study we demonstrated a potent effect of TRAIL-transduced DCs to ameliorate acute GVHD. A similar strategy may be also useful for Ag-specific immunosuppression in allogeneic organ transplantation, autoimmune diseases, and allergic diseases. Studies are now underway to address this possibility.

Acknowledgments

We thank K. Sato, Y. Sato, A. Takeuchi, and M. Yamamoto for excellent assistance.

Disclosures

The authors have no financial conflict of interest.

References

1. Lahm, A., A. Paradisi, D. R. Green, and G. Melino. 2003. Death fold domain interaction in apoptosis. *Cell Death Differ. 10:10.*
2. Smyth, M. J., K. Takeda, Y. Hayakawa, J. J. Peschon, M. R. van den Brink, and H. Yagita. 2003. Nature's TRAIL: on a path to cancer immunotherapy. *Immunity 18:1.*
3. Smyth, M. J., E. Cretney, K. Takeda, R. H. Wiltrout, L. M. Sedger, N. Kayagaki, H. Yagita, and K. Okumura. 2001. Tumor necrosis factor-related apoptosis-inducing ligand (TRAIL) contributes to interferon γ-dependent natural killer cell protection from tumor metastasis. *J. Exp. Med. 193:661.*
4. Takeda, K., Y. Hayakawa, M. J. Smyth, N. Kayagaki, N. Yamaguchi, S. Kakuta, Y. Iwakura, H. Yagita, and K. Okumura. 2001. Involvement of tumor necrosis factor-related apoptosis-inducing ligand in surveillance of tumor metastasis by liver natural killer cells. *Nat. Med. 7:94.*
5. Kayagaki, N., N. Yamaguchi, M. Nakayama, A. Kawasaki, H. Akiba, K. Okumura, and H. Yagita. 1999. Involvement of TNF-related apoptosis-inducing ligand in human CD4$^+$ T cell-mediated cytotoxicity. *J. Immunol. 162:2639.*
6. Song, K., Y. Chen, R. Goke, A. Wilmen, C. Seidel, A. Goke, B. Hilliard, and Y. Chen. 2000. Tumor necrosis factor-related apoptosis-inducing ligand (TRAIL) is an inhibitor of autoimmune inflammation and cell cycle progression. *J. Exp. Med. 191:1095.*
7. Lunemann, J. D., S. Waiczies, S. Ehrlich, U. Wendling, B. Seeger, T. Kamradt, and F. Zipp. 2002. Death ligand TRAIL induces no apoptosis but inhibits activation of human (auto)antigen-specific T cells. *J. Immunol. 168:4881.*
8. Lamhamedi-Cherradi, S. E., S. J. Zheng, K. A. Maguschak, J. Peschon, and Y. H. Chen. 2003. Defective thymocyte apoptosis and accelerated autoimmune diseases in TRAIL$^{-/-}$ mice. *Nat. Immunol. 4:255.*
9. Cretney, E., A. P. Uldrich, S. P. Berzins, A. Strasser, D. I. Godfrey, and M. J. Smyth. 2003. Normal thymocyte negative selection in TRAIL-deficient mice. *J. Exp. Med. 198:491.*
10. Hilliard, B., A. Wilmen, C. Seidel, T. S. Liu, R. Goke, and Y. Chen. 2001. Roles of TNF-related apoptosis-inducing ligand in experimental autoimmune encephalomyelitis. *J. Immunol. 166:1314.*
11. Banchereau, J., F. Briere, C. Caux, J. Davoust, S. Lebecque, Y. J. Liu, B. Pulendra, and K. Palucka. 2000. Immunobiology of dendritic cells. *Annu. Rev. Immunol. 18:767.*
12. Steinman, R. M., and M. C. Nussenzweig. 2002. Avoiding horror autotoxicus: the importance of dendritic cells in peripheral T cell tolerance. *Proc. Natl. Acad. Sci. USA 99:351.*
13. Morelli, A. E., and A. W. Thomson. 2003. Dendritic cells: regulators of alloimmunity and opportunities for tolerance induction. *Immunol. Rev. 196:125.*
14. Matsue, H., K. Matsue, M. Walters, K. Okumura, H. Yagita, and A. Takashima. 1999. Induction of antigen-specific immunosuppression by CD95L cDNA-transfected 'killer' dendritic cells. *Nat. Med. 5:930.*
15. Lu, L., W. C. Lee, T. Takayama, S. Qian, A. Gambotto, P. D. Robbins, and A. W. Thomson. 1999. Genetic engineering of dendritic cells to express immunosuppressive molecules (viral IL-10, TGF-β, and CTLA4Ig). *J. Leukocyte Biol. 66:293.*
16. Morita, Y., J. Yang, R. Gupta. K. Shimizu, E. A. Shelden, J. Endres, J. J. Mule, K. T. McDonagh, and D. A. Fox. 2001. Dendritic cells genetically engineered to express IL-4 inhibit murine collagen-induced arthritis. *J. Clin. Invest. 107:1275.*
17. Liu, Z., X. Xu, H. C. Hsu, A. Tousson, P. A. Yang, Q. Wu, C. Liu, S. Yu, H. G. Zhang, and J. D. Mountz. 2003. CII-DC-AdTRAIL cell gene therapy inhibits infiltration of CII-reactive T cells and CII-induced arthritis. *J. Clin. Invest. 112:1332.*
18. Shlomchik, W. D., M. S. Couzens, C. B. Tang, J. McNiff, M. E. Robert, J. Liu, M. J. Shlomchik, and S. G. Emerson. 1999. Prevention of graft versus host disease by inactivation of host antigen-presenting cells. *Science 285:412.*
19. Tsukada, N., T. Kobata, Y. Aizawa, H. Yagita, and K. Okumura. 1999. Graft-versus-leukemia effect and graft-versus-host disease can be differentiated by cytotoxic mechanisms in a murine model of allogeneic bone marrow transplantation. *Blood 93:2738.*
20. Schmaltz, C., O. Alpdogan, B. J. Kappel, S. J. Muriglan, J. A. Rotolo, J. Ongchin, L. M. Willis, A. S. Greenberg, J. M. Eng, J. M. Crawford, et al. 2002. T cells require TRAIL for optimal graft-versus-tumor activity. *Nat. Med. 8:1433.*
21. Sato, K., N. Yamashita, N. Yamashita, M. Baba, and T. Matsuyama. 2003. Regulatory dendritic cells protect mice from murine acute graft-versus-host disease and leukemia relapse. *Immunity 18:367.*
22. Sato, K., N. Yamashita, M. Baba, and T. Matsuyama. 2003. Modified myeloid dendritic cells act as regulatory dendritic cells to induce anergic and regulatory T cells. *Blood 101:3581.*
23. Kayagaki, N., N. Yamaguchi, M. Nakayama, K. Takeda, H. Akiba, H. Tsutsui, H. Okamura, K. Nakanishi, K. Okumura, and H. Yagita. 1999. Expression and function of TNF-related apoptosis-inducing ligand on murine activated NK cells. *J. Immunol. 163:1906.*
24. Nishimura, N., Y. Nishioka, T. Shinohara, H. Ogawa, S. Yamamoto, K. Tani, and S. Sone. 2001. Novel centrifugal method for simple and highly efficient adenovirus-mediated green fluorescence protein gene transduction into human monocyte-derived dendritic cells. *J. Immunol. Methods 253:113.*
25. Uno, K., T. Inukai, N. Kayagaki, K. Goi, H. Sato, A. Nemoto, K. Takahashi, K. Kagami, N. Yamaguchi, H. Yagita, et al. 2003. TNF-related apoptosis-inducing ligand (TRAIL) frequently induces apoptosis in Philadelphia chromosome-positive leukemia cells. *Blood 101:3658.*
26. Takeda, K., N. Yamaguchi, H. Akiba, Y. Kojima, Y. Hayakawa, J. E. Tanner, T. J. Sayers, N. Seki, K. Okumura, H. Yagita, et al. 2004. Induction of tumor-specific T cell immunity by anti-DR5 antibody therapy. *J. Exp. Med. 199:437.*
27. Fanger, N. A., C. R. Maliszewski, K. Schooley, and T. S. Griffith. 1999. Human dendritic cells mediate cellular apoptosis via tumor necrosis factor-related apoptosis-inducing ligand (TRAIL). *J. Exp. Med. 190:1155.*
28. Yu, Y., S. Liu, W. Wang, W. Song, M. Zhang, W. Zhang, Z. Qin, and X. Cao. 2002. Involvement of tumour necrosis factor-α-related apoptosis-inducing ligand in enhanced cytotoxicity of lipopolysaccharide-stimulated dendritic cells to activated T cells. *Immunology 106:308.*
29. Jo, M., T. H. Kim, D. W. Seol, J. E. Esplen, K. Dorko, T. R. Billiar, and S. C. Strom. 2000. Apoptosis induced in normal human hepatocytes by tumor necrosis factor-related apoptosis-inducing ligand. *Nat. Med. 6:564.*
30. Zheng, S.-J., P. Wang, G. Tsabary, and Y. H. Chen. 2004. Critical roles of TRAIL in hepatic cell death and hepatic inflammation. *J. Clin. Invest. 113:58.*

TCR Engagement Increases Hypoxia-Inducible Factor-1α Protein Synthesis via Rapamycin-Sensitive Pathway under Hypoxic Conditions in Human Peripheral T Cells[1]

Hiroshi Nakamura,* Yuichi Makino,* Kensaku Okamoto,* Lorenz Poellinger,† Kei Ohnuma,* Chikao Morimoto,* and Hirotoshi Tanaka[2]*

Peripheral T cells encounter rapid decrease in oxygen tension because they are activated by Ag recognition and migrate into inflammatory sites or tumors. Activated T cells, therefore, are thought to have such machineries that enable them to adapt to hypoxic conditions and execute immune regulation in situ. We have recently shown that survival of CD3-engaged human peripheral blood T cells is prolonged under hypoxic conditions and hypoxia-inducible factor-1 (HIF-1) and its target gene product adrenomedullin play a critical role for the process. It is also shown that hypoxia alone is not sufficient, but TCR-mediated signal is required for accumulation of HIF-1α in human peripheral T cells. In the present study, we showed that TCR engagement does not influence hypoxia-dependent stabilization but stimulates protein synthesis of HIF-1α, most possibly via PI3K/mammalian target of rapamycin system, and that expression of HIF-1α and its target genes is blocked by treatment with rapamycin. Since some of those gene products, e.g., glucose transporters and phosphoglycerokinase, are considered to be essential for glycolysis and energy production under hypoxic conditions and adequate immune reaction in T cells, this TCR-mediated synthesis of HIF-1α may play a pivotal role in peripheral immune response. Taken together, our results may highlight a novel aspect of downstream signal from Ag recognition by TCR and a unique pharmacological role of rapamycin as well. ***The Journal of Immunology,* 2005, 174: 7592–7599.**

Immune cells encounter rapid changes in oxygen tension as they develop and migrate into different compartments of the body (1). Especially peripheral T cells are activated by Ag recognition in inflammatory sites or in tumor, both of which are known to be hypoxic (2). Hypoxic environment is generally considered to be disadvantageous for cellular energy production and survival. It, therefore, appears to be rather paradoxical that activated T cells consume energy to synthesize adhesion molecules and cytokines and perform various functions including adhesion, migration, prolongation of survival and proliferation, cytokine secretion, and cytotoxicity (3). Given this, activated T cells should have such machineries that enable them to adapt for changes in oxygen tension and execute these functions in situ.

The transcription factor hypoxia-inducible factor-1 (HIF-1)[3] is generally believed to be a central regulator of the cellular response to hypoxia (4, 5). HIF-1 induces expression of the genes essential for adaptation to hypoxia including those for erythropoietin, glucose transporters, glycolytic enzymes, and vascular endothelial growth factor (VEGF), eliciting successful homeostatic regulation under hypoxic conditions. Moreover, genetic studies have clearly indicated the essential role of HIF-1α in regulation of inflammation and immune system. For example, genetic disruption of HIF-1α resulted in abnormal B cell development and autoimmunity (6), and selective deletion of HIF-1α gene in granulocytes and macrophages/monocytes was shown to lead to impairment of inflammatory responses such as motility, invasiveness, and bacterial killing of those cells in mice (7).

HIF-1 consists of two distinct basic helix-loop-helix PAS (Per/Arnt/Sim) transcription factors, HIF-1α and HIF-1β. HIF-1α is sensitive to oxygen levels, and, under normoxic conditions, several proline residues are hydroxylated by distinct prolyl hydroxylases and rapidly degraded via ubiquitin-proteasome pathway (4). However, under hypoxic conditions, HIF-1α subunit is stabilized and translocates into the nucleus, thereby homodimerizing with HIF-1β and binding to hypoxia-response element (HRE) DNA sequence on the promoter region of HIF-1 target genes to activate their transcription (8). In addition to this hypoxia-dependent mechanism, recent studies have demonstrated non-hypoxic pathways for regulation of HIF-1α activity (9, 10) and multiple regulatory mechanisms of HIF-1α protein level, may enable cells to adapt to diverse alteration of environments and preserve homeostasis in a tissue-dependent manner. For example, receptor-mediated regulation of HIF-1α expression is thought to be cell and signal specific, and a number of reports have suggested that receptor-mediated factors such as growth factors, hormones, and cytokines induce HIF-1α protein expression through various signalings including PI3K/mammalian target of rapamycin (mTOR) pathway (11–15).

*Division of Clinical Immunology, Advanced Clinical Research Center, Institute of Medical Science, University of Tokyo, Tokyo, Japan; and †Department of Cell and Molecular Biology, Nobel Medical Institute, Karolinska Institute, Stockholm, Sweden

Received for publication October 26, 2004. Accepted for publication March 18, 2005.

The costs of publication of this article were defrayed in part by the payment of page charges. This article must therefore be hereby marked *advertisement* in accordance with 18 U.S.C. Section 1734 solely to indicate this fact.

[1] This work was supported in part by grants from the Ministry of Education, Science, Technology, Sports and Culture, the Ministry of Health, Labor, and Welfare of Japan, the Takeda Science Foundation, the Uehara Memorial Foundation, the Vehicle Racing Commemorative Foundation, Novartis Foundation, and the Cell Science Research Foundation.

[2] Address correspondence and reprint requests to Dr. Hirotoshi Tanaka, Division of Clinical Immunology, Advanced Clinical Research Center, Institute of Medical Science, University of Tokyo, 4-6-1, Shirokanedai, Minato-ku, Tokyo 108-8639, Japan. E-mail address: hirotnk@ims.u-tokyo.ac.jp

[3] Abbreviations used in this paper: HIF-1, hypoxia-inducible factor-1; VEGF, vascular endothelial growth factors; HRE, hypoxia response element; mTOR, mammalian target of rapamycin; ADM, adrenomedullin; GLUT, glucose transporter; PGK1, phosphoglycerate kinase-1; CHX, cycloheximide.

Copyright © 2005 by The American Association of Immunologists, Inc.

0022-1767/05/$02.00

Rapamycin is an immunosuppressive agent clinically approved for use in kidney transplant patients and additional applications are being considered in autoimmune and chronic inflammatory diseases (16). Rapamycin binds to FK506-binding protein 12, and this complex targets mTOR and inhibits T cell response to IL-2 to progress G_1 to S phase (17). On the other hand, it has been noticed that rapamycin suppresses the growth of certain tumors (18, 19). For example, rapamycin inhibits metastatic tumor growth and angiogenesis in mouse model and this anti-angiogenic activity is shown to link to a decrease in production of VEGF (20). Furthermore, Majumder et al. (21) have clearly indicated that the antitumor effect of rapamycin is, at least in part, mediated by inhibition of mTOR-dependent HIF-1α expression using Akt-dependent prostate intraepithelial neoplasia.

We have recently shown that survival of CD3-engaged human peripheral blood T cells is prolonged under hypoxic conditions, and that HIF-1 and its target gene product adrenomedullin (ADM) play a critical role in the process. Interestingly, it is also shown that hypoxia alone is not sufficient but additional TCR-mediated signal is required for sufficient accumulation of HIF-1α in human peripheral T cells (22). However, underlying mechanisms of TCR-dependent HIF-1α accumulation in human peripheral T cells remain unclear. In the present study, we demonstrated that Ab-mediated TCR engagement does not influence hypoxia-dependent stabilization but stimulates protein synthesis of HIF-1α, most possibly via PI3K/mTOR system, in peripheral blood T cells. Moreover, expression of HIF-1α and its target gene expression was blocked by treatment with rapamycin. Taken together, our results may highlight a novel aspect of downstream signal from Ag recognition by TCR and a unique pharmacological role of rapamycin as well.

Materials and Methods

Abs and reagents

The mAb against human CD3 (UCHT1) was purchased from BD Pharmingen. Anti-human HIF-1α (Ab463) and anti-human HIF-1β Abs were obtained from Abcam. Abs against Akt and phosphorylated Akt at threonine 308 were purchased from Cell Signaling Technologies. Recombinant human IL-2 was obtained from PeproTech and PHA-M from Sigma-Aldrich. Other chemicals were purchased from Sigma-Aldrich unless otherwise specified.

Cell culture and activation of peripheral T cells

Fresh PBMC were prepared from heparinized blood of healthy volunteers by Ficoll-Paque Plus (Amersham Biosciences) density gradient centrifugation and suspended in RPMI 1640 medium (Sigma-Aldrich) supplemented with 10% FBS and antibiotics. Adherent cells were removed by incubation on plastic dishes for 1 h at 37°C, and the rest of the cells were separated on nylon wool columns to obtain T cell rich fraction. For activation, T cell blasts were generated by stimulation of the T cell fraction (1×10^6 cells/ml) with 5 μg/ml PHA-M for 48 h. The mitogen was then washed out, and the cells were maintained in the medium containing 10 ng/ml recombinant human IL-2. For additional experiments, the cells were washed three times with PBS and used as T cells in the present study. CD3 engagement of the cells (1×10^6 cells/ml) was performed in the presence of 10 ng/ml IL-2 on 6-well plates coated with anti-CD3 mAb (5 μg/ml), and exposure of the cells to various oxygen concentrations was conducted as described previously (22).

Western blotting

Immunodetection of HIF-1α protein was performed as described previously (23). Briefly, whole cell extracts of T cells were prepared in lysis buffer consisting of 25 mM HEPES, 100 mM NaCl, 5 mM EDTA, 100 μM orthovanadate, and 0.5% Triton X-100, pH 7.9, followed by centrifugation at 14,000 rpm for 30 min at 4°C. Whole cell extract (60 μg) was separated with SDS-PAGE and electrically transferred onto polyvinylidene fluoride filters. The filters were incubated with anti-HIF-1α Ab at a dilution of 1:1000 in PBS containing 1% nonfat milk at 4°C overnight, followed by anti-mouse Ig-HRP conjugates (Amersham Biosciences) in the same buffer. Immunocomplexes were visualized using ECL as recommended by the manufacturer (Amersham Biosciences).

Northern blotting

Total RNA isolation from human peripheral T cells and Northern blot analysis were performed as described elsewhere (13). In brief, 2×10^7 T cells were stimulated with anti-CD3 Ab under normoxic or hypoxic conditions and harvested. Total RNA was isolated from T cells by guanidine isothiocyanate lysis/phenol chloroform extraction, followed by removal of contaminating DNA, and 10-μg aliquots of RNA were fractionated by electrophoresis in 1.5% agarose 2.2 M formaldehyde gels, transferred to Hybond N membranes (Amersham Biosciences), and hybridized with a ^{32}P-labeled human HIF-1α cDNA probe.

Metabolic labeling

A total of 1×10^7 of T cells were incubated in a 6-well plate with or without 5 μg/ml anti-CD3 Ab. The cells were pretreated with or without MG132 in methionine-free RPMI 1640 medium. [^{35}S]Methionine-cysteine was added to a final concentration of 0.3 mCi/ml, and the cells were pulse labeled for 30 min and then harvested. Whole cell extracts were prepared with RIPA buffer (50 mM Tris-HCl, 150 mM NaCl, 1 mM EDTA, 1% Triton X-100, 0.1% SDS, 0.1% sodium deoxycholate). Cell extract was precleared with protein A-Sepharose for 1 h. Anti-HIF-1α Ab was added to the supernatant and rotated overnight at 4°C. Twenty microliters of 50% slurry of protein A-Sepharose equilibrated with RIPA buffer was added to the mixture, rotated for 2 h at 4°C, pelleted and washed four times with RIPA buffer. Precipitated materials were eluted by boiling in SDS sample buffer. Samples were separated with SDS-PAGE, and the gel was vacuum dried and visualized by autoradiography.

RT-PCR analysis

First strand cDNA was synthesized using 2 μg of DNase-treated total RNA as a template in 20 μl of reaction mixture containing 50 mM Tris-HCl (pH 8.3), 3 mM $MgCl_2$, 10 mM DTT, 75 mM KCl, 1 mM dNTP, 0.1 mM oligo(dT) primer, and 50 U of Superscript II (Invitrogen Life Technologies) at 42°C for 50 min. PCR was conducted in a total volume of 30 μl in a mixture composed of 10 mM Tris-HCl (pH 8.3), 50 mM KCl, 1.5 mM $MgCl_2$, 200 μM dNTP, 0.25 μM each of the sense and antisense primers, and 1 U of ExTaq DNA polymerase (TaKaRa). The amount of cDNA, as judged by the intensity of the amplified β-actin signal, was comparable among the preparations. Amplification by 27 cycles of 94°C for 30 s, 50°C for 30 s, and 72°C for 1 min was performed after 3 min of denaturing of the samples at 94°C and shown to be within linear range or non-saturated conditions for each primers amplification. Identities of the PCR products were confirmed by DNA sequencing. Primer pairs for amplification of each gene are as follows: HIF-1α, sense: 5'- CTGTGATGAGGCTTACCAT CAGC-3', antisense: 5'-CTCGGCTAGTTAGGGTACACTTC-3'; ADM, sense: 5'-GCGATCCGACTCACCAATAC-3'; antisense: 5'-TGGATCC TGAGTCGAAGTCT-3'; glucose transporter-1 (GLUT-1), sense: 5'-CTT TCTCCAGCCAGCAATGA-3', antisense: 5'-TGGATCCTGAGTCGAA GTCT-3'; GLUT-3, sense: 5'-GATGCTGGAGAGGTTAAGGT-3', antisense: 5'- ACTTCCACCCAGAGCAAAGT-3'; phosphoglycerate kinase-1 (PGK1), sense: 5'-CGAGCCAGCCAAAATAGAAGC-3', antisense: 5'-TCAAACAGAGAAGTGCCAATC-3'; VEGF, sense: 5'-TGCCT

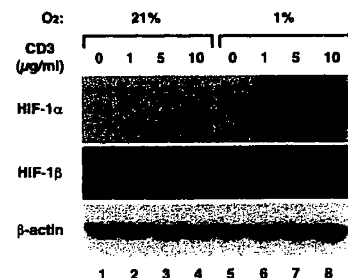

FIGURE 1. TCR engagement-mediated accumulation of HIF-1α protein expression in peripheral T cells. Human peripheral blood T cells were incubated in the absence or presence of increasing concentrations of immobilized anti-CD3 mAb (CD3) for 12 h under 21 or 1% oxygen concentration. Whole cell extracts were prepared and immunoblotting was performed with anti-HIF-1α, HIF-1β, and β-actin Abs as described in *Materials and Methods*.

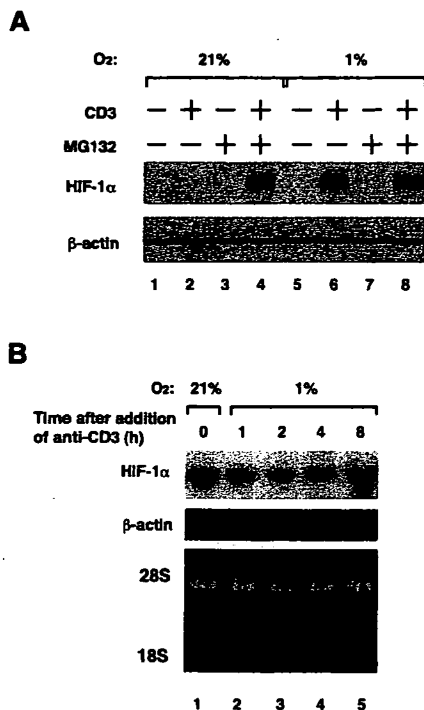

FIGURE 2. Effect of CD3/TCR engagement on protein stability and steady-state level of mRNA of HIF-1α. *A*, Immunoblots for HIF-1α. Human peripheral blood T cells were cultured in the absence or presence of 5 μg/ml immobilized anti-CD3 mAb (CD3) or 5 μM MG132 for 12 h under 21 or 1% oxygen concentration as indicated. Protein levels of HIF-1α and β-actin were determined as described in *Materials and Methods*. *B*, Northern blot analysis for HIF-1α mRNA. Human peripheral blood T cells were cultured in the absence or presence of 5 μg/ml immobilized anti-CD3 mAb under 21 or 1% oxygen concentration for the indicated time periods. After isolation of total RNA, Northern blot for HIF-1α (*top*) or β-actin (*middle*) was performed as described in *Materials and Methods*. As a loading control, ethidium bromide-stained gel was presented in the bottom.

TGCTGCTCTACCTCC-3′, antisense: 5′-TCACCGCCTCGGCTTGT CAC-3′; IL-2, sense: 5′-ATGTACAGGATGCAACTCCTGTCTT-3′; antisense: 5-AGCTGTTTCAGTTCTGTGGCCTTCT-3′; β-actin, sense: 5′-CCTCGCCTTTGCCGATCC-3′, antisense: 5′-GGATCTTCATGAG GTAGTCAGTC-3′.

Transient transfection and luciferase assay

Jurkat T cell line stably expressing constitutive active form of HIF-1α or mock-DNA were grown to confluence in RPMI 1640 medium plus 10% FBS and other supplements. Cells were transfected with plasmid DNA containing promoter-reporter constructs by an electroporation method. Briefly, cells were washed twice with Opti-MEM (Invitrogen Life Technologies) and resuspended in the same medium at a concentration of 2 × 10^7 cells/ml. Cell suspension was placed in a electroporation cuvette (Gene Pulser; Bio-Rad) followed by adding 5 μg of HRE reporter plasmid DNA. The electroporation was conducted at a capacitance of 950 microfarads and 250 V. After electroporation, the cells were kept on ice for 10 min and resuspended in 10 ml of complete RPMI 1640 medium, and incubated for 12 h at 37°C in 5%. Then cells were further incubated for 36 h in either normoxic or hypoxic conditions. Luciferase enzyme activity was determined using a luminometer (Promega), and relative light units were normalized to the protein amount determined with BCA protein assay reagent according to the manufacturer's instructions (Pierce).

Results

We first analyzed the effect of TCR-mediated signals on protein levels of HIF-1α in human peripheral T cells under hypoxic conditions. For that purpose, human peripheral T cells were treated with various doses of an immobilized mAb against CD3 under normoxic (21%) or hypoxic (1%) conditions and Western blot was performed to determine HIF-1α protein. Under normoxic condition, HIF-1α was not detected even in the presence of relatively high concentration of anti-CD3 mAb. However, under hypoxic condition, TCR/CD3 engagement up-regulated protein expression of HIF-1α in a concentration-dependent manner but did not that of HIF-1β (Fig. 1).

It has recently been reported that HIF-1α expression is regulated at multiple levels including stability/degradation, protein synthesis/translation, and transcription, by a distinct set of upstream signals, dependent on cells or tissues (see introduction). Therefore, we addressed at which level HIF-1α expression is regulated by

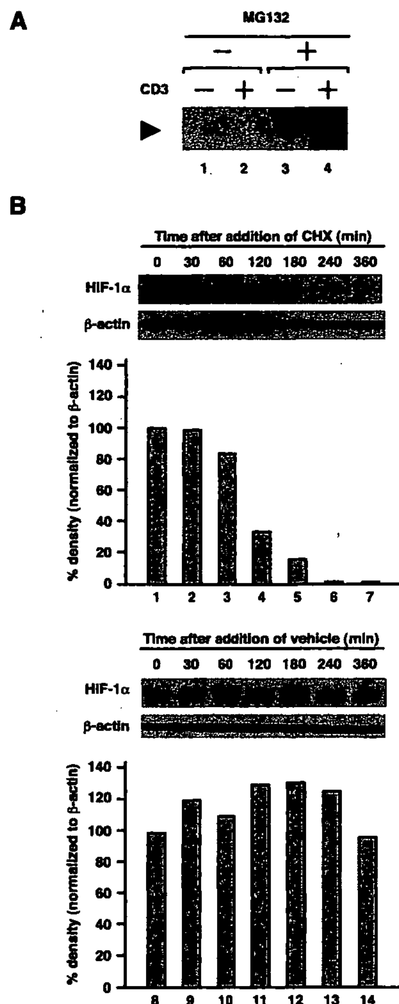

FIGURE 3. TCR/CD3 engagement-dependent HIF-1α protein expression is regulated at the level of protein synthesis. *A*, Metabolic labeling analysis. Serum-starved human peripheral blood T cells were preincubated in the absence or presence of 5 μM MG132 or immobilized anti-CD3 Ab in methionine-free medium for 2 h under normoxic condition as indicated and pulse labeled with 0.3 mCi/ml [^{35}S]methionine-cysteine for 30 min. After isolation of whole cell extracts, HIF-1α was affinity purified by immunoprecipitation and separated by 8% SDS-PAGE as described in *Materials and Methods*. The gel was dried and ^{35}S-labeled HIF-1α protein was detected by autoradiography. *B*, Effect of a protein synthesis inhibitor CHX on HIF-1α protein expression. Human peripheral blood T cells were incubated for 12 h in the absence or presense of 5 μM MG132 and incubated in the presence (*top panel*) or absence (*bottom panel*) of 100 μM CHX for the indicated time periods. HIF-1α and β-actin were analyzed in immunoblots as described in *Materials and Methods*. Density of the bands was measured with NIH IMAGE 1.62 software being normalized to β-actin. Results are shown as relative density (percentage compared with the sample harvested after preincubation with MG132).

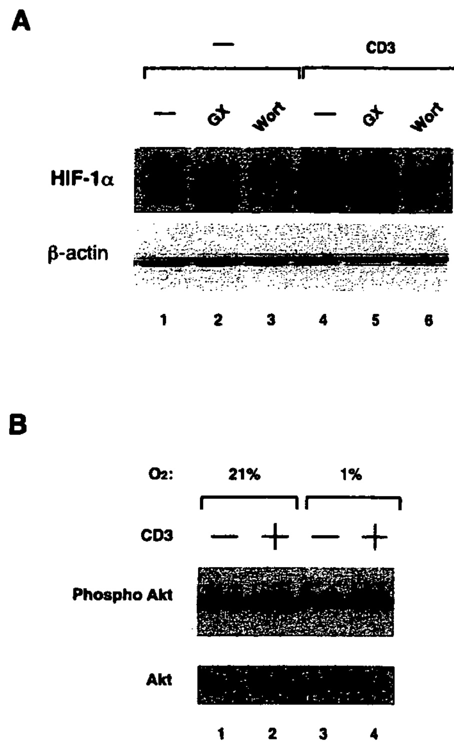

FIGURE 4. Involvement of PI3K activation in TCR/CD3-dependent HIF-1α protein expression. *A*, Immunoblots for HIF-1α. Human peripheral blood T cells were incubated for 12 h in the absence or presence of 10 μM GF109203X (GX), 100 nM wortmannin (Wort), and immobilized anti-CD3 Ab (CD3). HIF-1α and β-actin proteins were detected in immunoblots as described in *Materials and Methods*. *B*, Akt phosphorylation. Human peripheral blood T cells were incubated for 12 h in the absence or presence of immobilized anti-CD3 mAb (CD3) under 21 or 1% oxygen concentration for 12 h. Thr308-phosphorylated form and total Akt protein was detected in immunoblots.

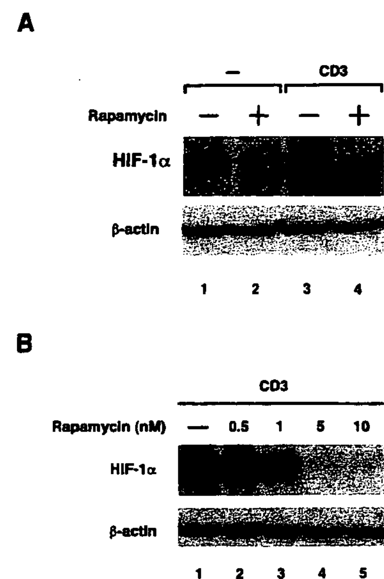

FIGURE 5. Rapamycin inhibits TCR/CD3 engagement-dependent HIF-1α protein expression. Human peripheral blood T cells were incubated for 12 h in the absence or presence of various concentrations of rapamycin (10 nM in *A*, and 0.5, 1, 5, and 10 nM in *B*), or anti-CD3 mAb (CD3) under hypoxic conditions (1% O_2), and HIF-1α or β-actin were detected in immunoblots.

TCR/CD3 ligation in peripheral blood T cells. Concerning protein stability/degradation, treatment of T cells with a proteasome inhibitor MG132 alone failed to restore HIF-1α protein, whereas that in combination with anti-CD3 stimulation successfully restored HIF-1α expression under normoxic condition. Combination of hypoxic treatment and TCR/CD3 ligation up-regulated HIF-1α expression to similar levels, and addition of MG132 did not further increase HIF-1α levels (Fig. 2*A*). These results may indicate that TCR/CD3 engagement does not influence protein stability of HIF-1α and acts via a distinct mechanism concerning the increment of HIF-1α protein accumulation.

Next we tested the effect of TCR ligation on the steady-state level of HIF-1α mRNA in peripheral blood T cells. T cells were stimulated with anti-CD3 mAb for the indicated time period under hypoxic conditions, and cellular contents of HIF-1α mRNA was determined using Northern blot analysis. Expression of HIF-1α mRNA appeared to be unaffected at any time point after application of anti-CD3 mAb (Fig. 2*B*), indicating that alteration in steady-state level of HIF-1α mRNA is unlikely to be responsible for TCR ligation-mediated accumulation of HIF-1α protein in T cells under hypoxic conditions.

Given these results, we examined a role of protein synthesis machinery. For that purpose, we first performed metabolic labeling analysis. Peripheral blood T cells were incubated with anti-CD3 mAb under normoxic conditions in the presence or absence of MG132 then pulse-labeled by means of [^{35}S]methionine-cysteine incorporation followed by immunoprecipitation of HIF-1α. As shown in Fig. 3*A*, ^{35}S-incorporated HIF-1α was clearly detected not in the cells without stimulation but in those treated with anti-CD3 mAb in the presence of MG132 (Fig. 3*A*), indicating that in addition to the inhibition of degradation, an up-regulation of HIF-1α protein synthesis by TCR ligation contributes to HIF-1α protein accumulation. To further confirm this issue, T cells were treated with anti-CD3 mAb in the presence of MG132 under normoxic conditions, then a protein synthesis inhibitor cycloheximide (CHX) was added and the culture was further continued for the indicated time period. HIF-1α protein levels were markedly decreased after addition of CHX, whereas T cells without CHX treatment showed persistent expression of HIF-1α for up to 6 h (Fig. 3*B*). Decrease in HIF-1α protein level started as early as 60 min after treatment with CHX, and HIF-1α protein was hardly detectable after 4 h of treatment with CHX (Fig. 3*B*). These results suggest that detectable HIF-1α protein accumulation requires continuous protein synthesis via CD3/TCR stimulation even when proteasomal degradation is inhibited either under hypoxic conditions or in the presence of MG132.

Because it is shown that HIF-1α protein synthesis is up-regulated mainly via PI3K/mTOR pathway in, for example, cancer cells (see Introduction), we tested the possibility that TCR/CD3 ligation-mediated HIF-1α expression involves PI3K/mTOR pathway as well. For that purpose, we examined the effect of PI3K inhibitor wortmannin, comparing PKC inhibitor GF109203X. It is revealed that not GF109203X but wortmannin completely shuts down HIF-1α expression even under hypoxic condition (Fig. 4*A*). To test the effect of oxygen concentration and TCR/CD3 ligation on PI3K activity, we determined the phosphorylated form of PI3K downstream target Akt. Fig. 4*B* clearly demonstrates that TCR/CD3 ligation does not significantly alter protein levels of Akt but promotes its phosphorylation, and oxygen concentration does not affect the amount of either form of Akt. We next examined the effect of a specific mTOR inhibitor rapamycin on HIF-1α accumulation in peripheral blood T cells. As anticipated, rapamycin completely inhibited the induction of HIF-1α protein expression in anti-CD3-stimulated T cells under hypoxic conditions (Fig. 5*A*).